

High Frequency Radio Oceanography:

Principles, technology and applications

The *radlab* group:

Pierre Flament, Lindsey Benjamin, Johanna Saavedra, Philip Moravcik, Maël Flament, Bénédicte Dousset (University of Hawai'i Manoa)

Xavier Flores (Universidad Autónoma de Baja California)

Cédric Chavanne (Université du Québec à Rimousky)

Antony Kirincich, Ian Fernandez (Woods Hole Oceanographic Institution)

Charina Repollo, Aiko Del Rosario (University of the Philippines Diliman)

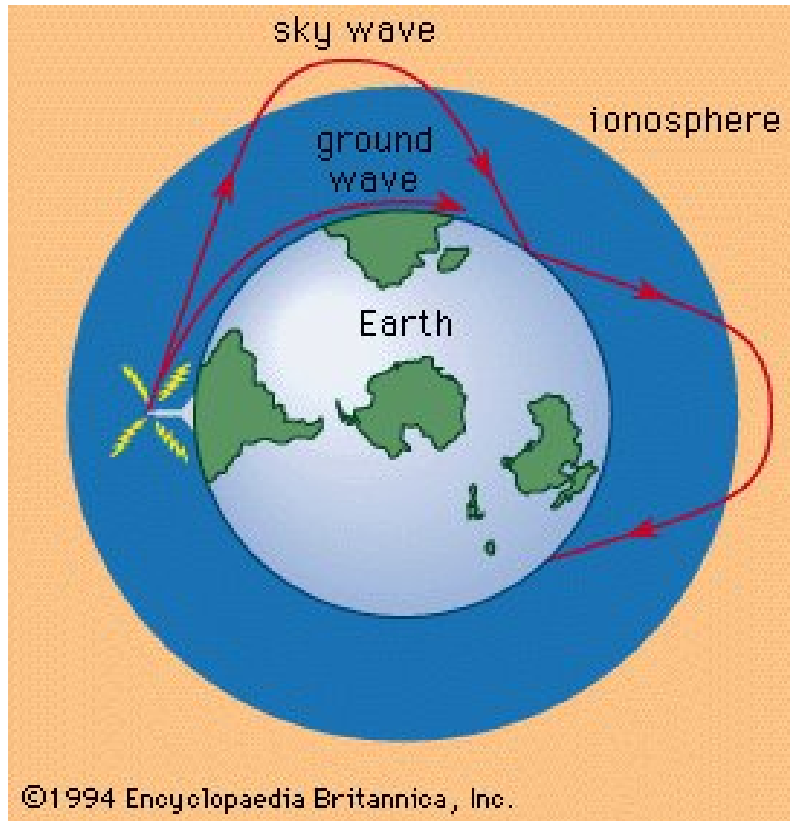
Louis Marié (IFREMER)

Huan Meng Chang, Hao Yuan Cheng, Đào Duy Toàn, Hwa Chien (National Central University Taiwan)

Peter Milne, John McLean (D-Tacq Solutions Ltd.)

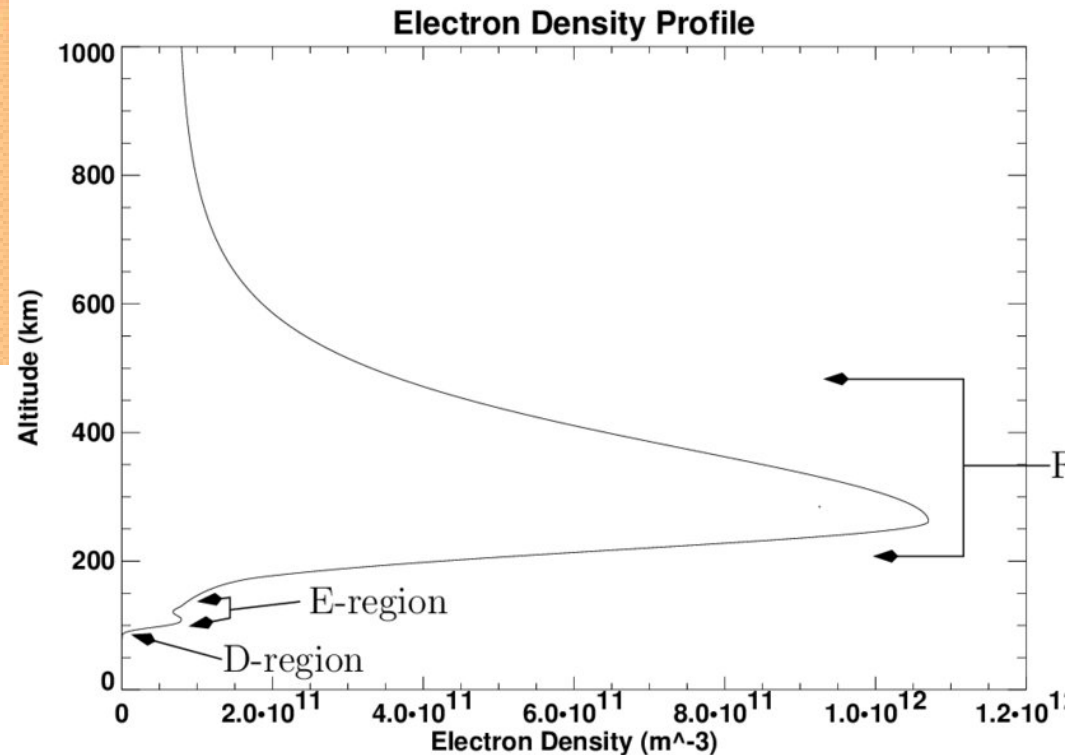
<https://www.oceanphysics.org/>

Electromagnetic propagation over conductive ocean



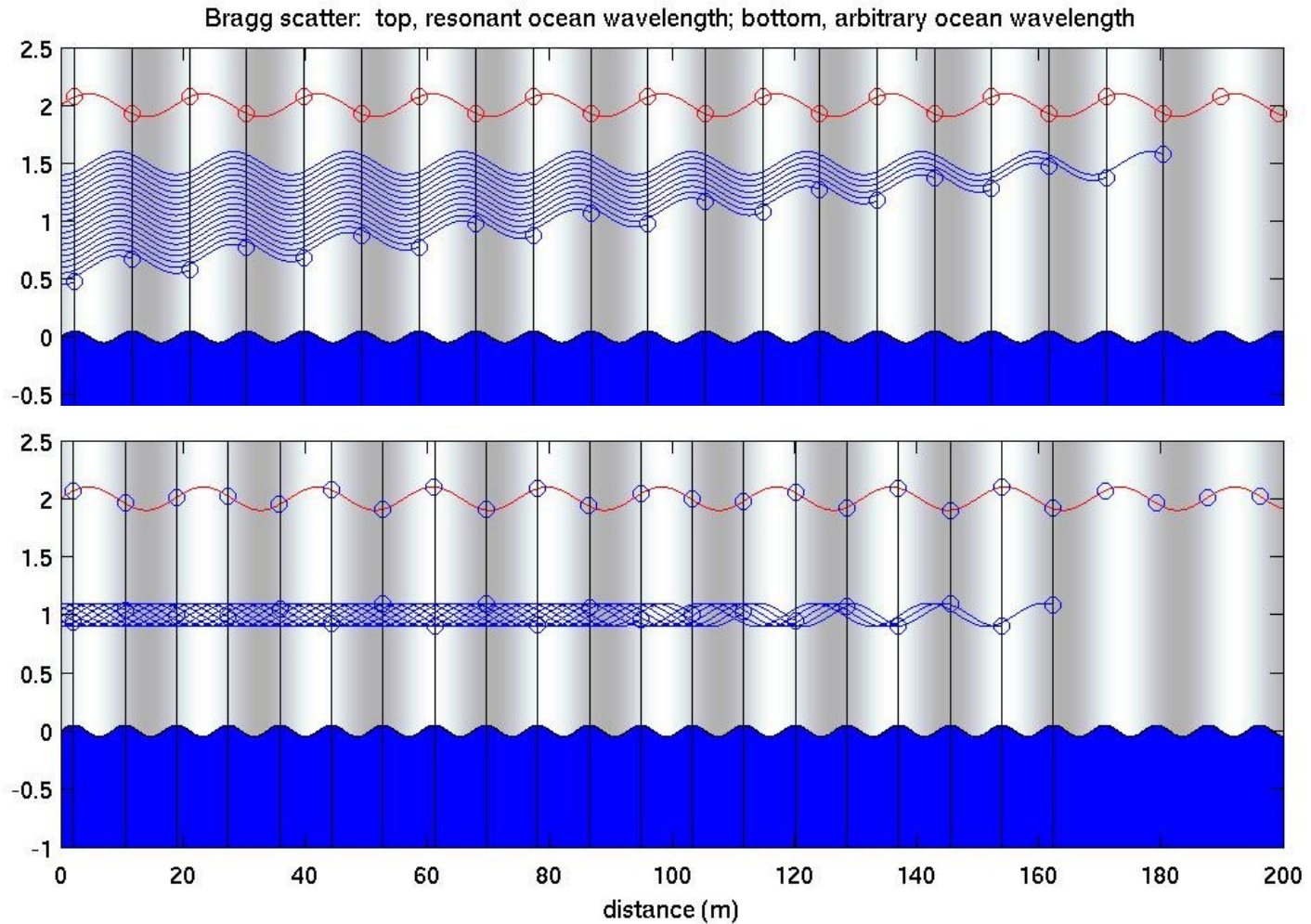
Conductivity:

- sea water $4 \text{ } \Omega/\text{m}$
- limestone $0.005 \text{ } \Omega/\text{m}$



Bragg-scattering from a water surface

Ocean Wavelength = $\frac{1}{2}$ Radio Wavelength



UH Generic High Frequency Doppler Radar specifications

Modulation	FMCW linear chirp
Operating Frequency Range	from 3 MHz to 30 MHz
Transmitted RF-Power	typically 3-5 W, max. 50 W
Range	50 km/ 25 NM @ 27 MHz 100 km/ 50 NM @ 16 MHz 260 km/ 140 NM @ 8 MHz
Range Resolution	depends on authorized bandwidth $c/2B$ 1.5km@ 100kHz, 150m @ 1MHz (voice 3kHz)
Azimuthal Resolution	better than 2 degrees

Current deployments of UH Generic HF radars:

- *Hawai'i, the Pacific Island Observing System (feeding into HFRnet):*
 - 5 radars at 13.5, 16 and 26.5 MHz operating on Oahu, since 2009
 - 2 radars at 16 and 24.5 MHz operating on Hawai'i, since 2012
 - 2 solar-powered radars at 13.5 MHz in Guam and Rota, starting 2025
- *Mexico (UABC):*
 - 3 radars at 24.5-26.5 MHz, covering Bahia de Todos Santos (Ensenada), installed 2015
 - 2 long-range radars at 8 MHz range up to 250 km offshore Baja California, installed 2016
 - 15 long-range radars at 7-8 MHz, covering the Gulf of Mexico, installed 2018
- *New England (WHOI):*
 - 10 radars at 16 MHz mapping the New England shelf, starting 2018
- *Luzon strait (UPD-MSI, with TORI):*
 - 3 long-range radars at 8 MHz, collaboration Philippines/Taiwan/Hawaii, 2019-2023
- *Quebec (ISMER):*
 - 2 mobile solar-powered radars at 16 MHz deployed in the St Lawrence estuary, since 2018
- *France (IFREMER):*
 - 1 long-range radar at 4.5 MHz over the southern Bay of Biscay, since 2021
- *Taiwan (NCU; NAMR; TORI; IHMT)*
 - 21 radars at 25-30 MHz covering harbors around TW, since 2018

The Helical Antenna*

JOHN D. KRAUS†, SENIOR MEMBER, IRE

Summary—The helix is a fundamental form of antenna of which loops and straight wires are limiting cases. When the helix is small compared to the wavelength, radiation is maximum normal to the helix axis. Depending on the helix geometry, the radiation may, in theory, be elliptically, plane, or circularly polarized.

When the helix circumference is about 1 wavelength, radiation may be maximum in the direction of the helix axis and circularly polarized or nearly so. This mode of radiation, called the axial or beam mode, is generated in practice with great ease, and may be dominant over a wide frequency range with desirable pattern, impedance, and polarization characteristics. The radiation pattern is

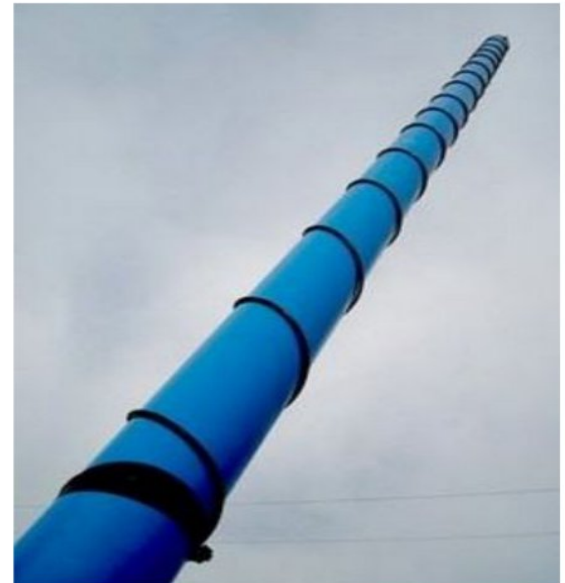
maintained in the axial mode over wide frequency ranges because of a natural adjustment of the phase velocity of wave propagation on the helix. The terminal impedance is relatively constant over the same frequency range because of the large initial attenuation of waves on the helix. The conditions for circular polarization are analyzed, and the importance of the array factor in determining the radiation pattern of a long helix is discussed.

INTRODUCTION

A HELIX is a fundamental geometric form. It has applications in many branches of physics and engineering. For example, in mechanical systems the helix or coil spring is a familiar structure; in electrical systems, a helical conductor or inductor is a common type of circuit element; and in many dynamic phenom-

* Decimal classification: R125.1×R326.61. Original manuscript received by the Institute, June 7, 1948. Presented in part, 1948 IRE National Convention, New York, N. Y., March 23, 1948.

† Department of Electrical Engineering, Ohio State University, Columbus, Ohio.



The transmit antennas are normal-mode helical monopoles (Kraus, J.D., "The Helical Antenna", *Proc. I.R.E.* 1949 pp. 263-272). They consist of an AWG-16 vertical wire of length $\lambda/4$ wound over a mast of height $\lambda/8$ and diameter $\lambda/300$, a 3-loop tuning air-coil, and a network of 4 underground radials of length $\lambda/4$ (λ is the electromagnetic wavelength). The air-coil diameter is adjusted to achieve resonance using a standard commercial VSWR meter.

Baler (Ph.) Receiving Array 8 MHz range 260 km



Penghu island TW 32 antennas range 40 km @ 26.5 MHz



Frequency-modulated homodyne radar

- Δt is travel time to & return from range
- Δf is frequency in FFT that gives range
- Shorter times and lower frequencies are closer ranges
- Maximum range indicates a maximum time and maximum frequency
- 150 km R, 100 kHz B, 1/3 s Tchirp:
 - $\Delta t = 2R / c = 1 \text{ ms}$
 - Chirp rate = $B / T_{\text{chirp}} = 300 \text{ kHz/s}$
 - $\Delta f = \Delta t * R_{\text{chirp}} \sim 300 \text{ Hz}$
 - Minimum F_s for Nyquist = 600 Hz

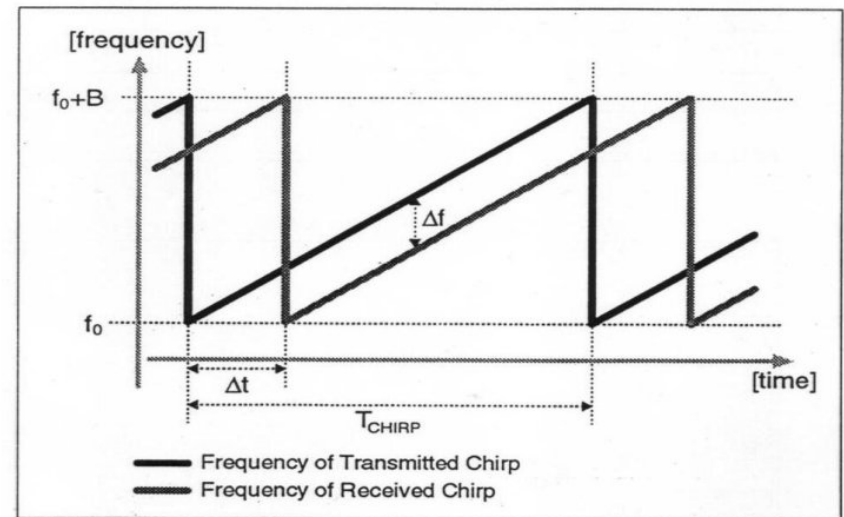


Figure 2: Range resolution using a frequency chirp.

Radial currents

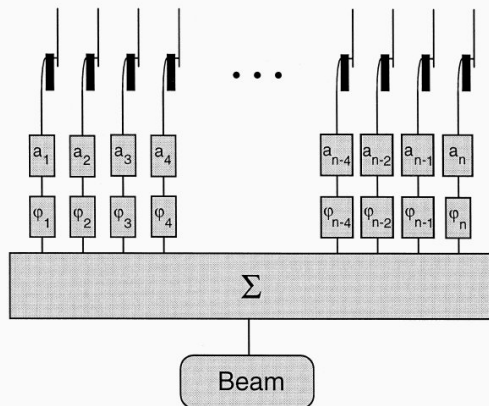
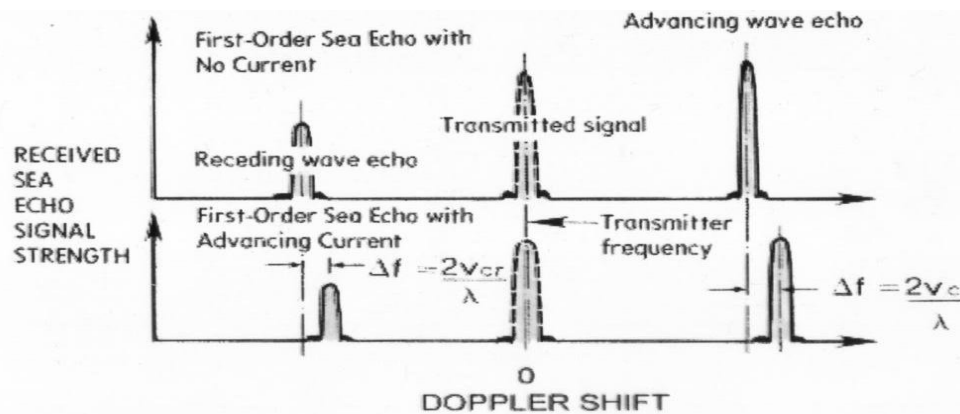
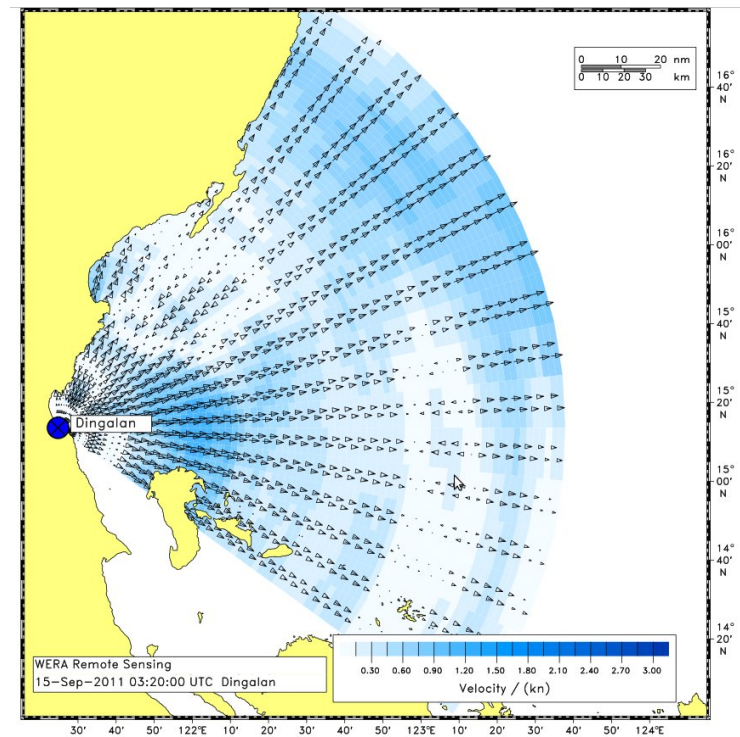
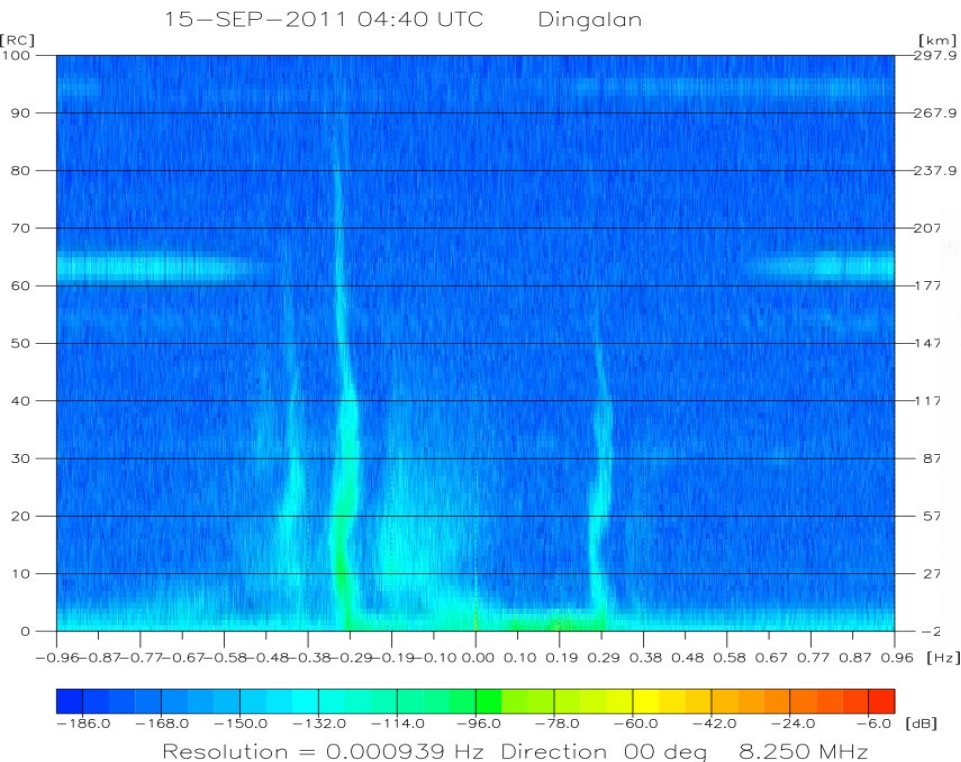
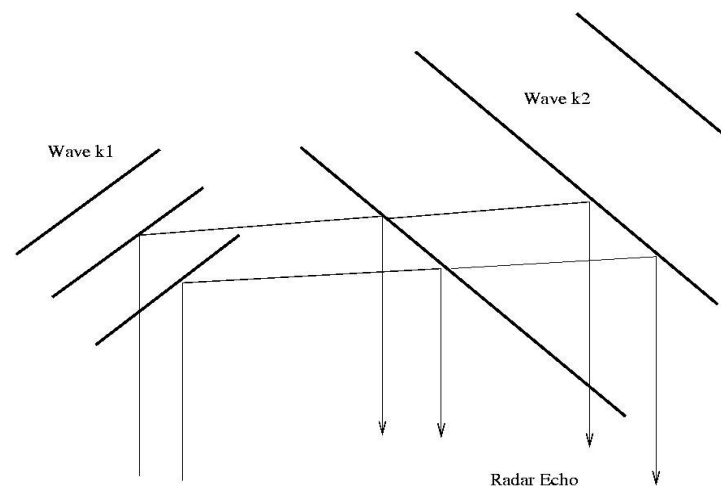
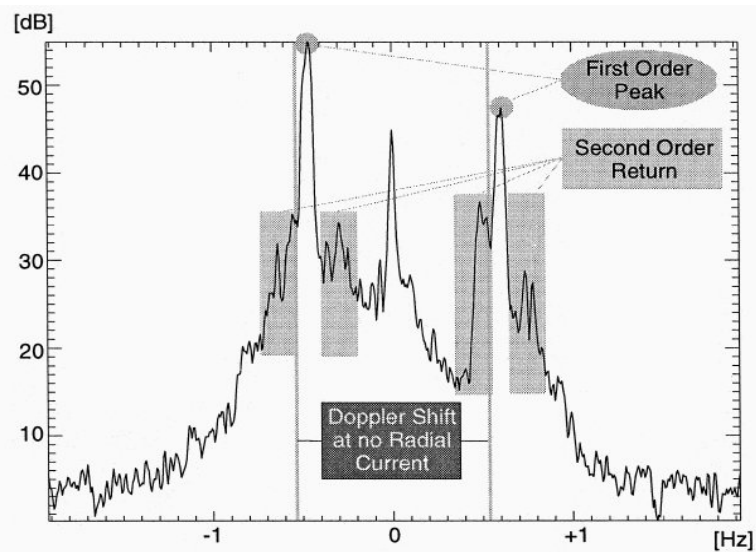
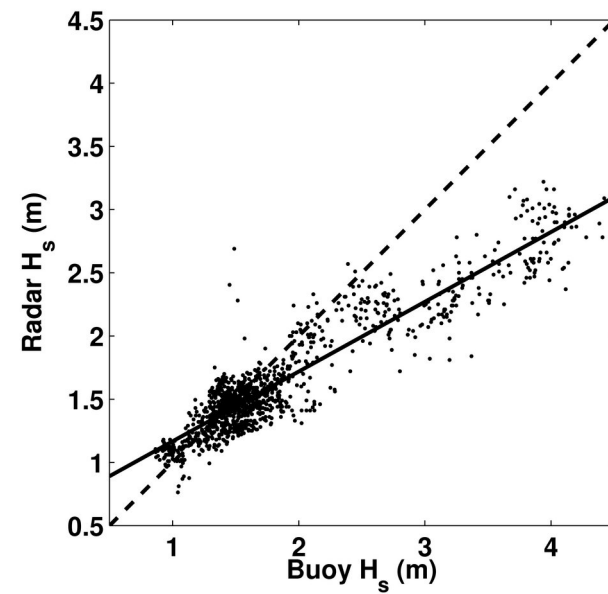
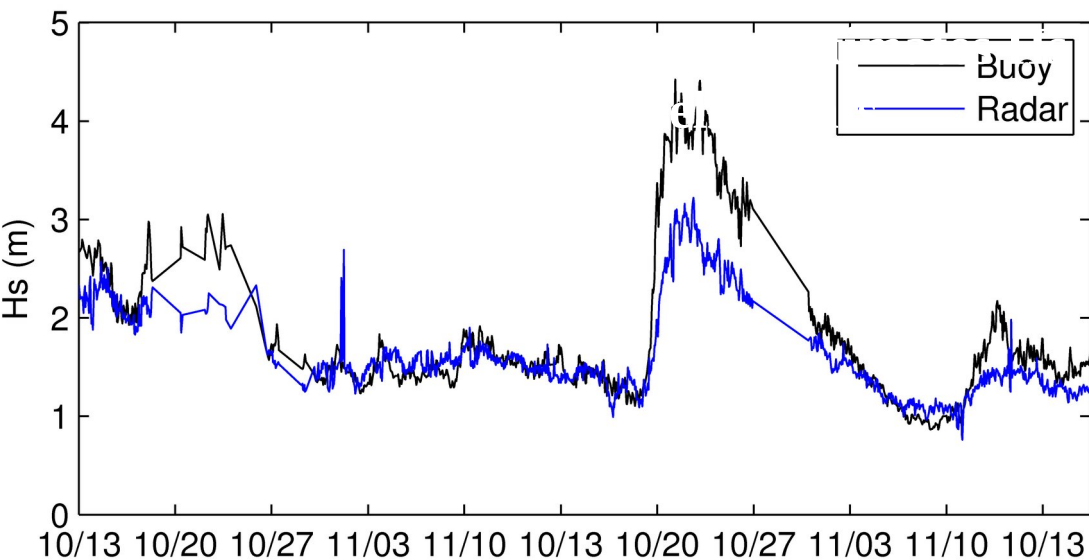


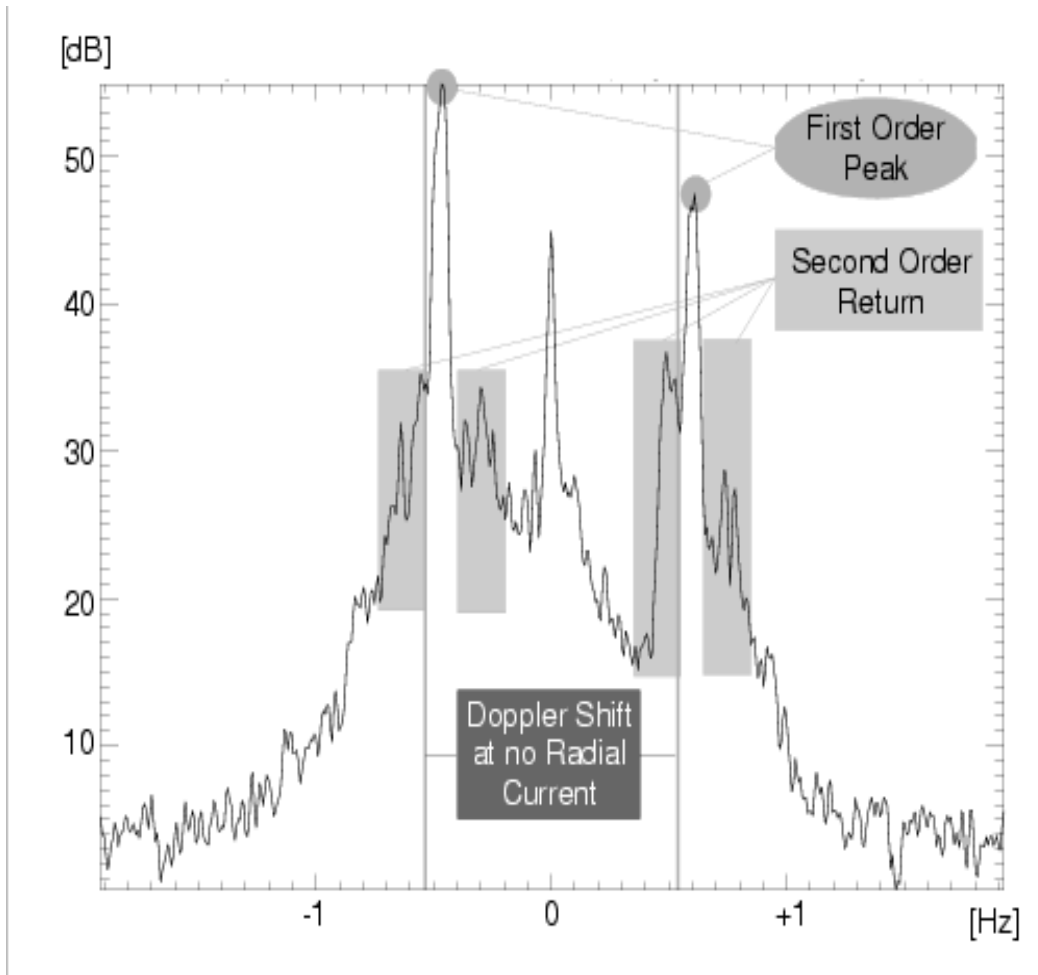
Fig. 10. Principle of beamforming. After weighing by a_i and phase shifting by ϕ_i the signals of n receive antennas are added.



Significant waveheight (H_s): buoy vs. HF radar



wind direction from HF radar



[Gurgel et al., 1999]

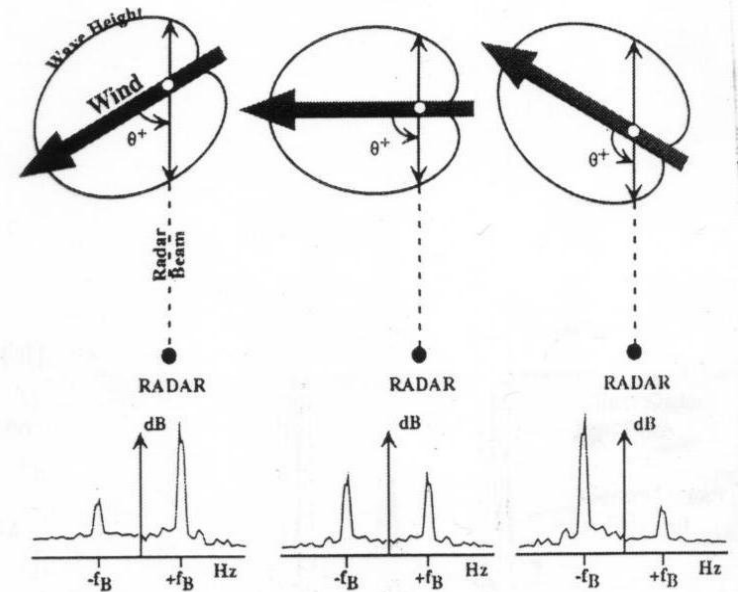


Fig. 1: Sample distributions of surface wave energy as a function of angle relative to the wind direction for cases with wind blowing toward (left), at right angles to (middle), and away from (right) the radar look direction. Sample backscatter spectra below show relative heights of the approaching (+) and receding (-) Bragg peaks for each case and θ^* denotes the angle between the wind and the approaching wave directions.

[Fernandez et al. 1997]

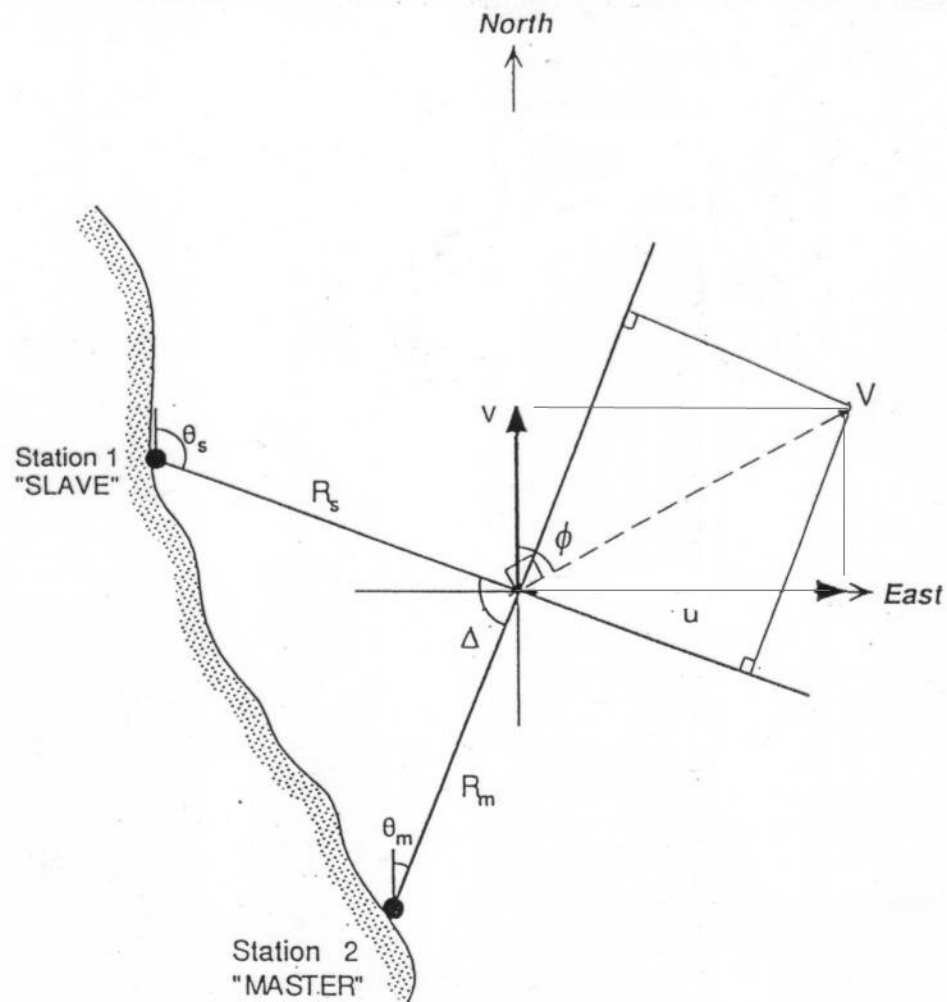
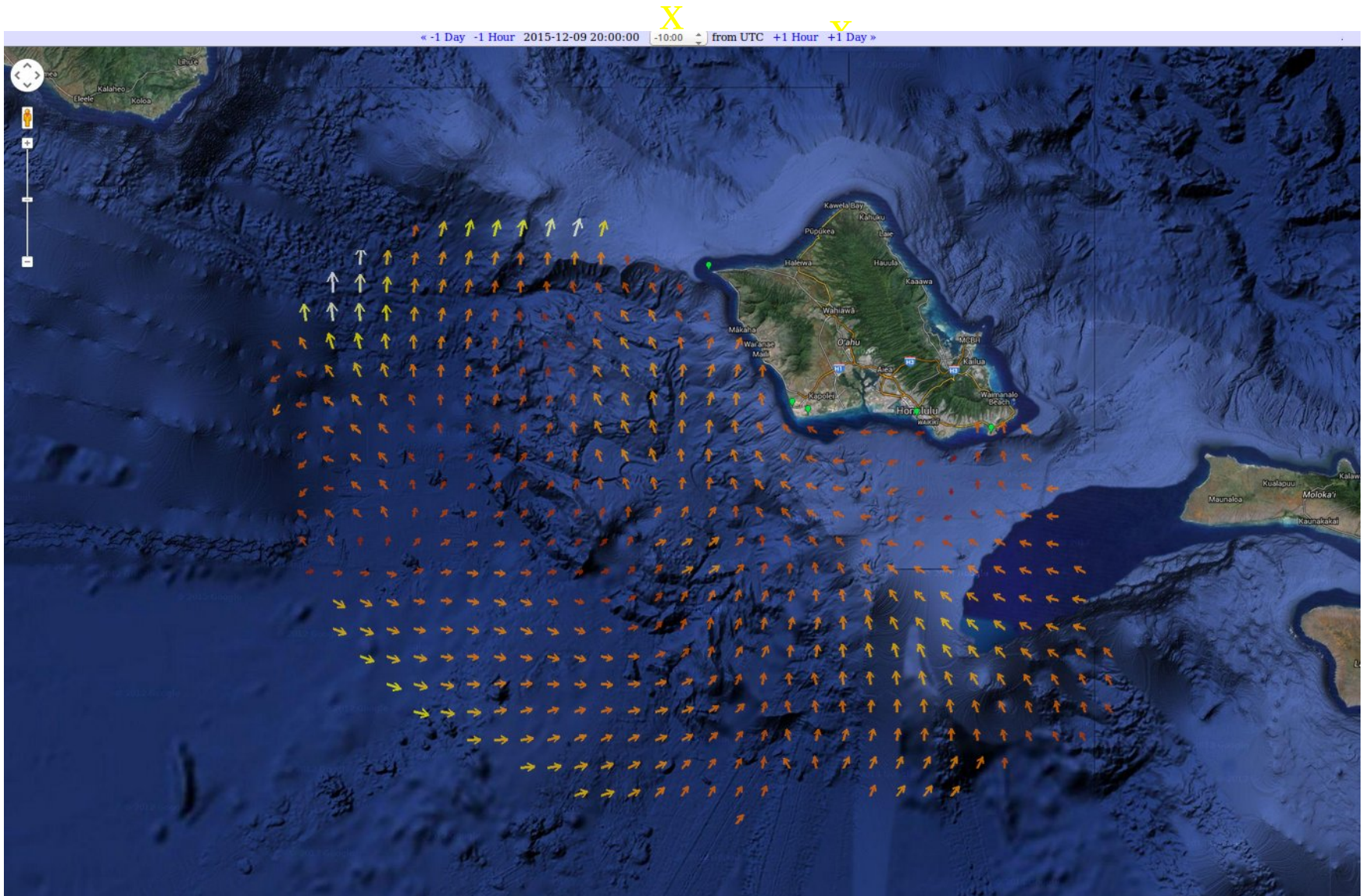


Figure 2. Schematic for determining the resulting vector current from velocity components of two intersecting radials.

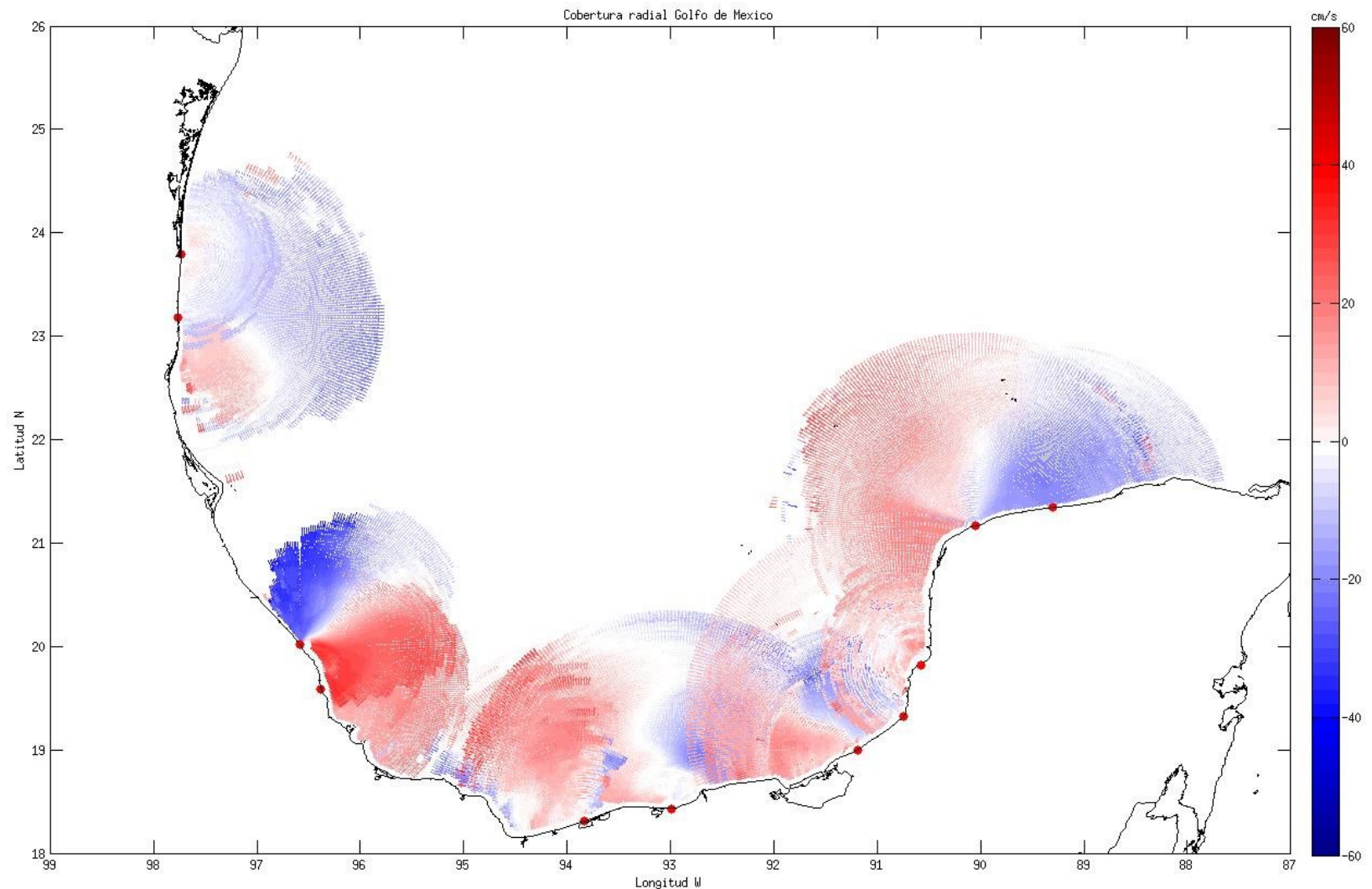
University of Hawaii Pacific Ocean Observing System hourly currents^X

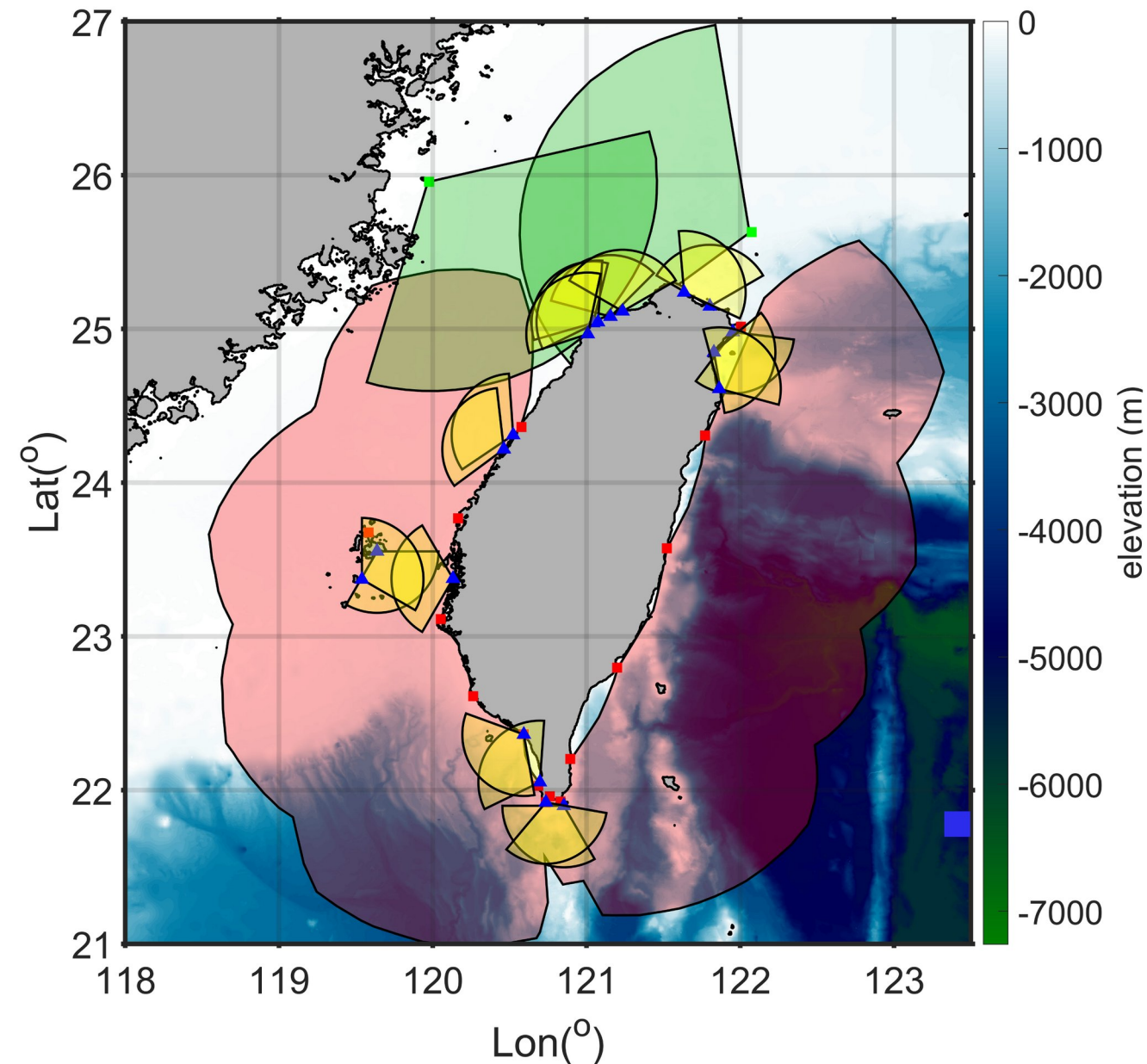


HF radar network for the Gulf of Mexico

20 radars, 6-8 MHz

with Universidad Autonoma de Baja California





Taiwan HF Radar Coverage and Bathymetry Map.



國家海洋研究院
National Academy of Marine Research

▲ 12 UH-GHFDR BF



▲ 5 UH-GHFDR BF

■ 2 CWA BF



Transportation Technology Research Center

▲ 2 UH-GHFDR BF

TORI NAR Labs 國家實驗研究院
台灣海洋科技研究中心
Taiwan Ocean Research Institute

■ 14 CODAR DF

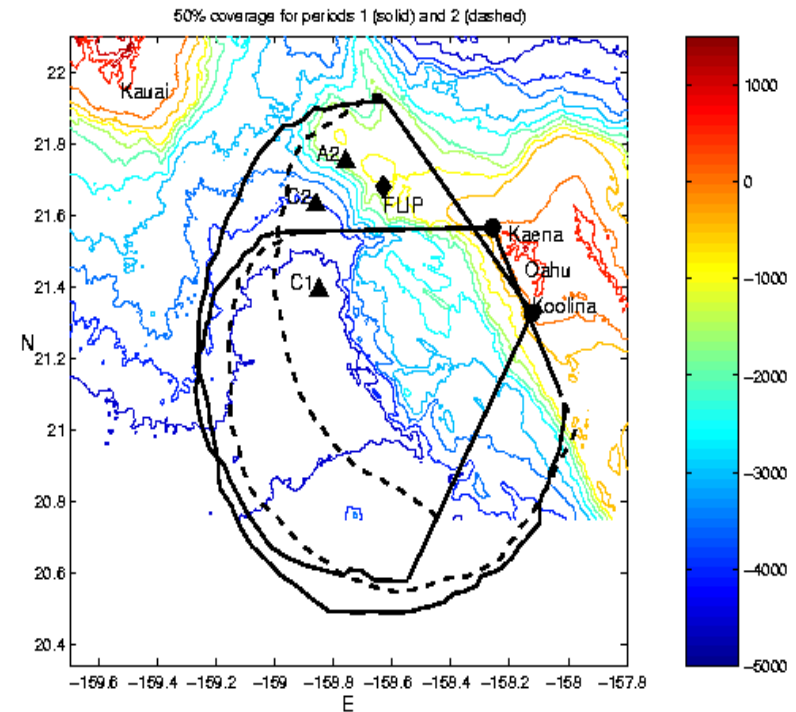
■ 2 UH-GHFDR DF

Validation:

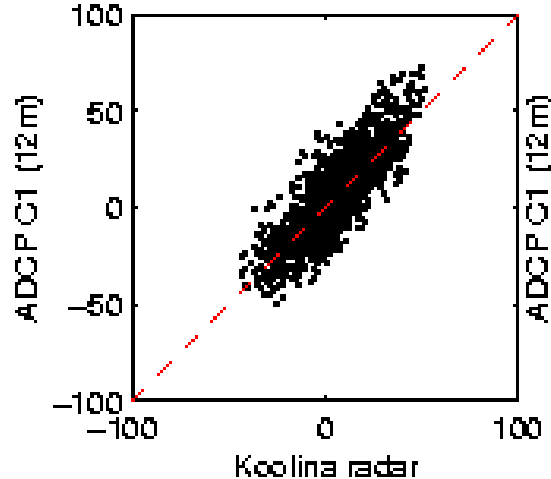
High Frequency Radar Currents
(16 MHz, 1 m)

vs.

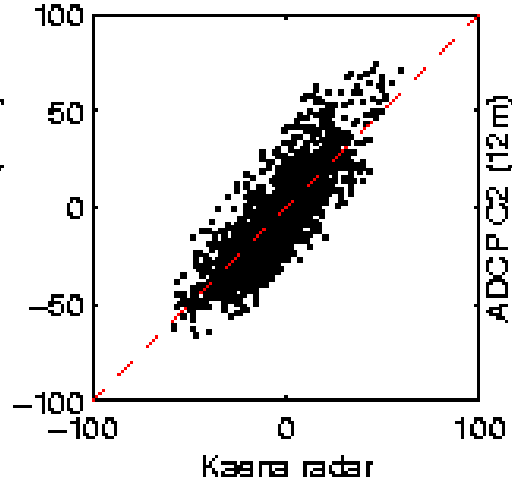
Acoustic Doppler Current meters
(300 kHz, 12 m)



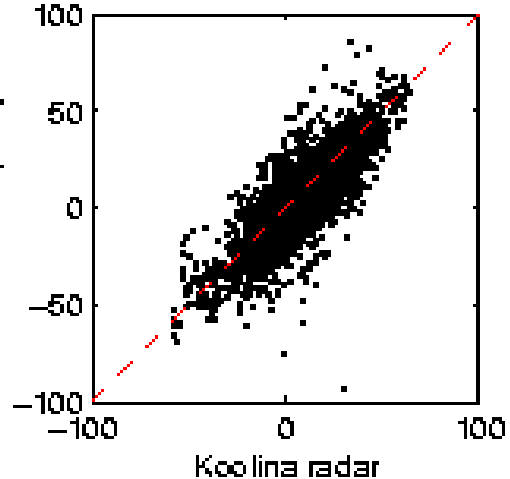
$r = 0.94$, $\text{med} = 0.41$, $\text{rms} = 12.15$



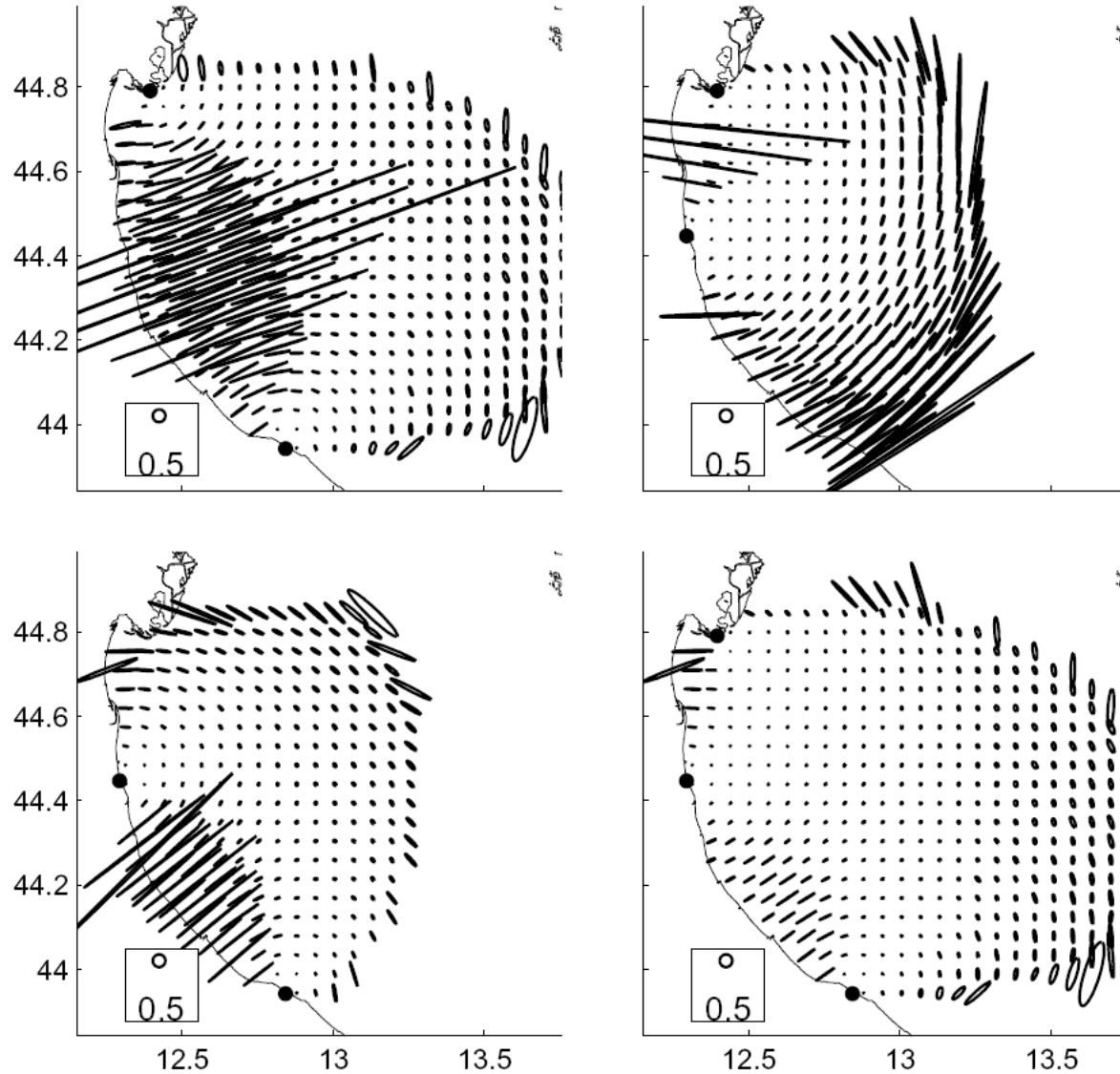
$r = 0.83$, $\text{med} = -1.52$, $\text{rms} = 13.97$



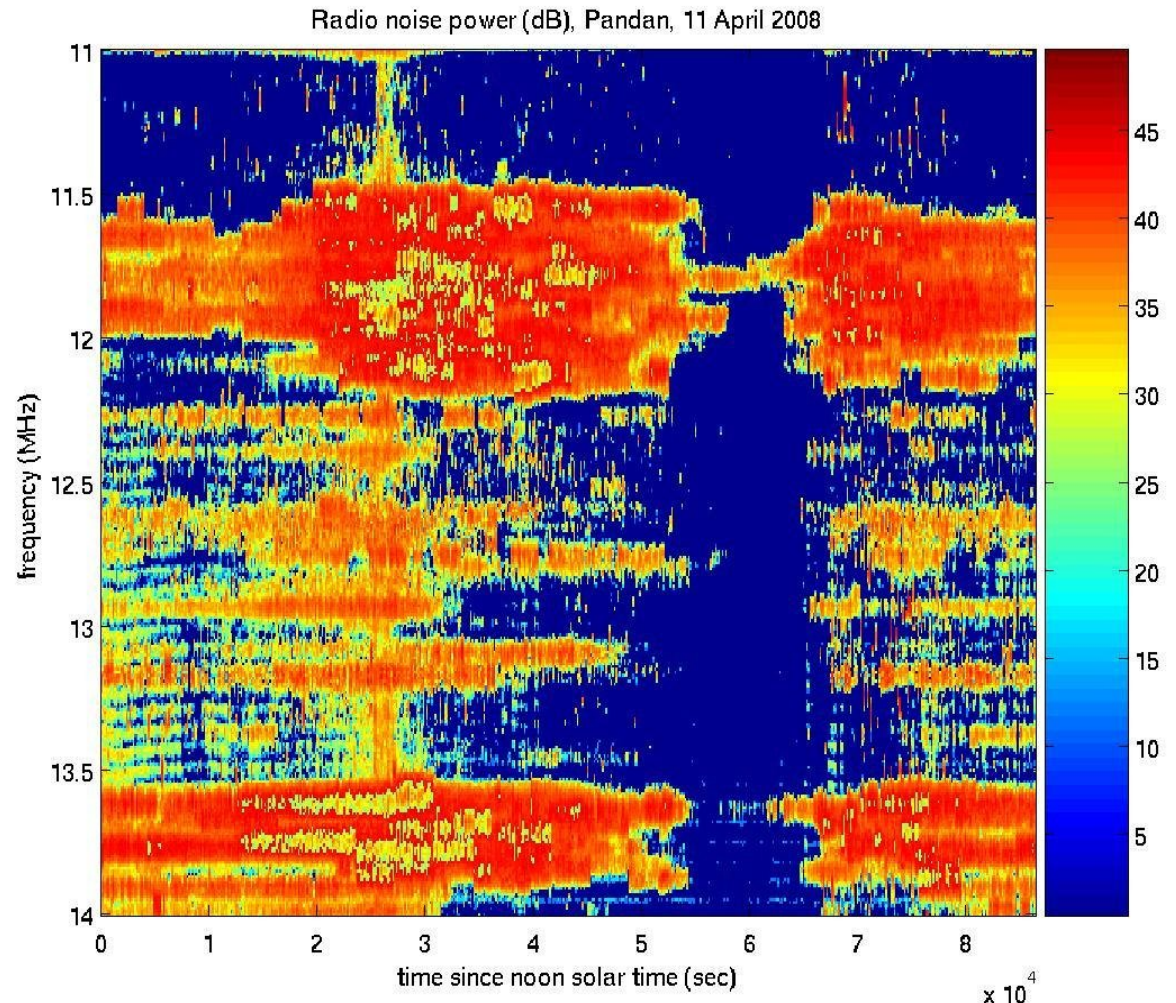
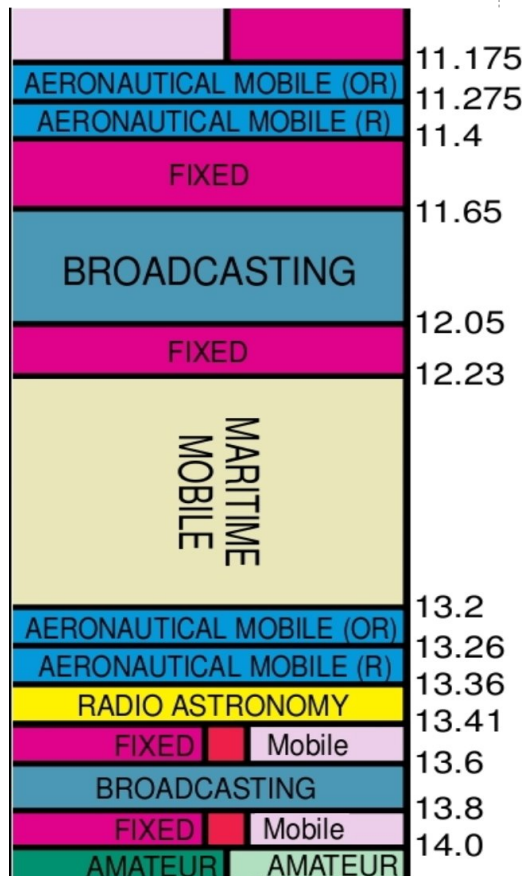
$r = 0.89$, $\text{med} = -3.71$, $\text{rms} = 13.06$

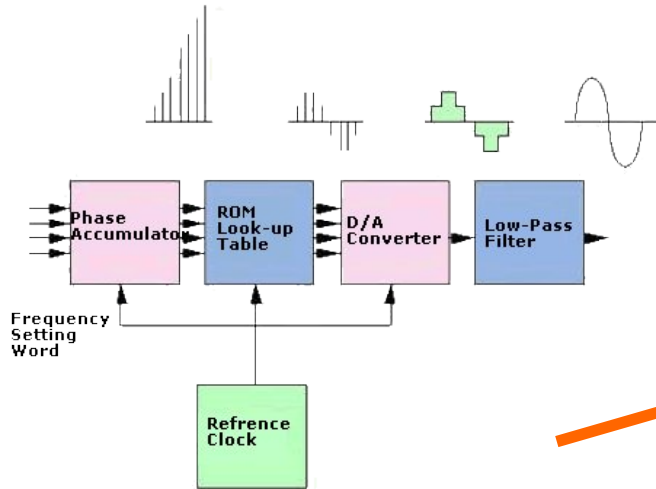


Caveat 1: Geometric Dilution Of Precision (GDOP)



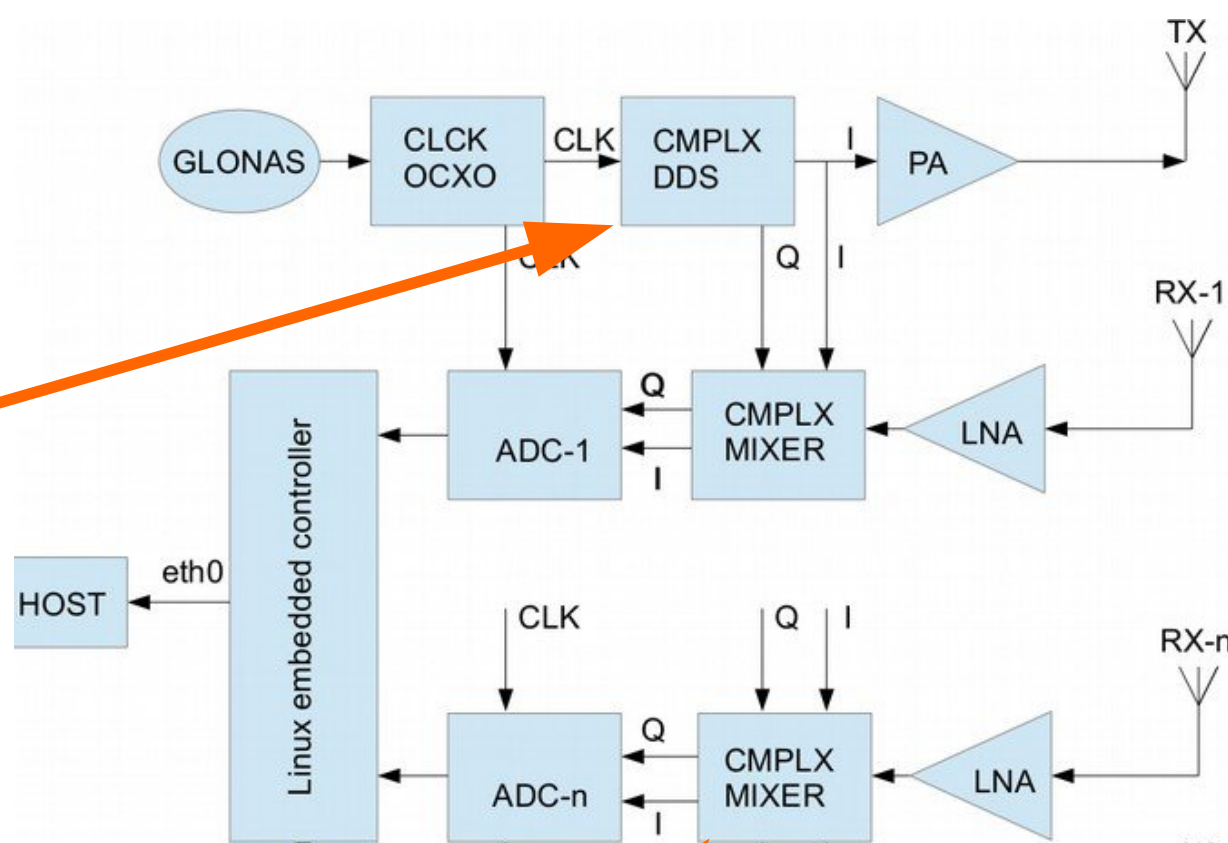
Caveat 2: interference from ionosphere-reflected transmitters





Direct Digital Synthesizer

Homodyne HF radars principle of operation

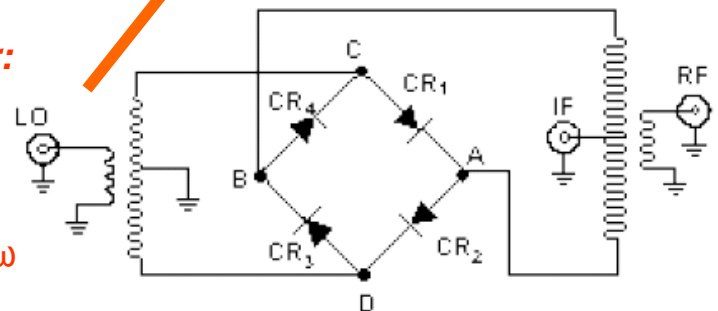


Double-Balanced Mixer/quadrature detector:

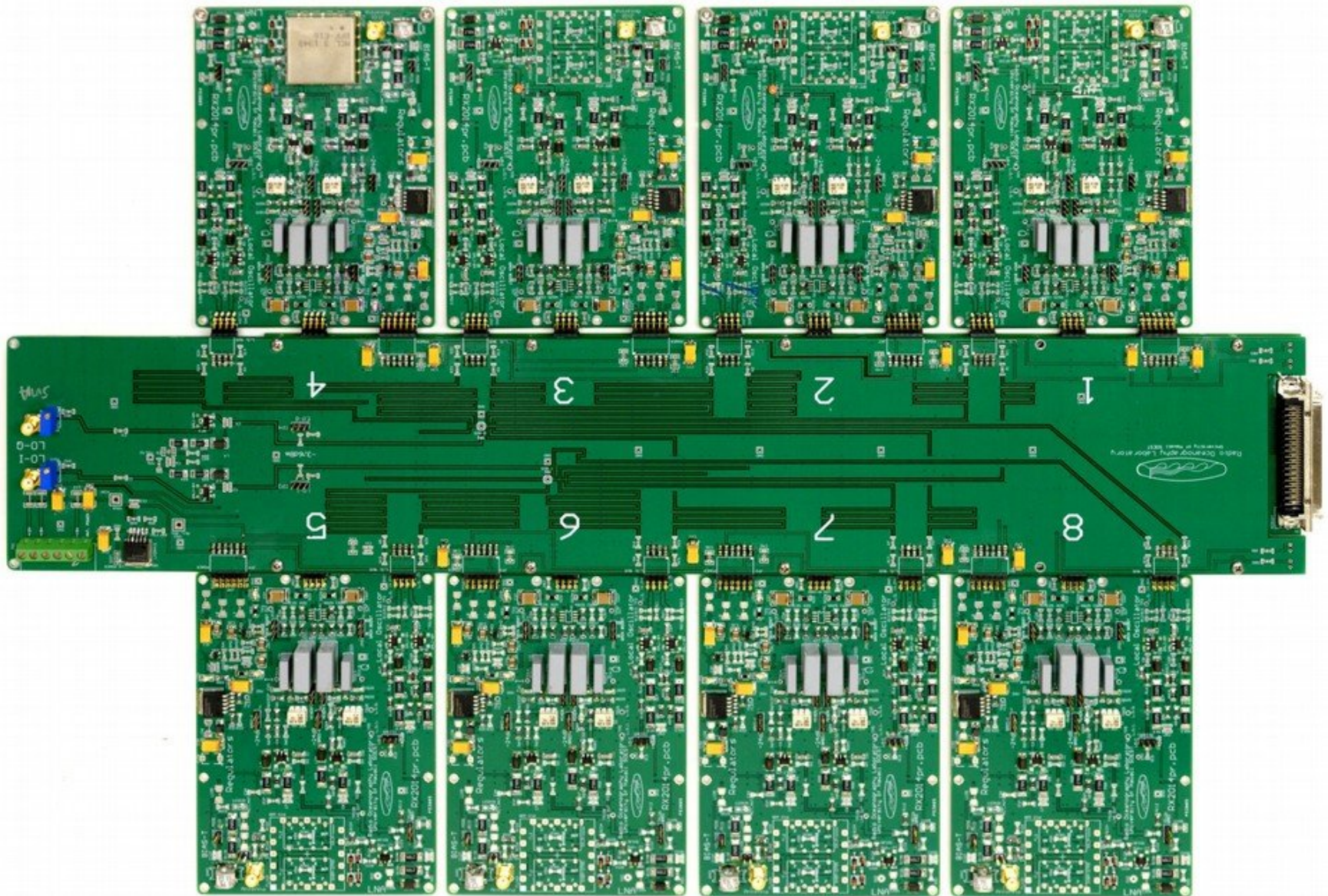
$$I: 2 \sin x \sin y = \cos (x-y) - \cos (x+y)$$

$$Q: 2 \sin x \cos y = \sin (x-y) + \sin (x+y)$$

if $x = (\omega + \Delta \omega) t$ and $y = \omega t$ then $x - y = \Delta \omega t$

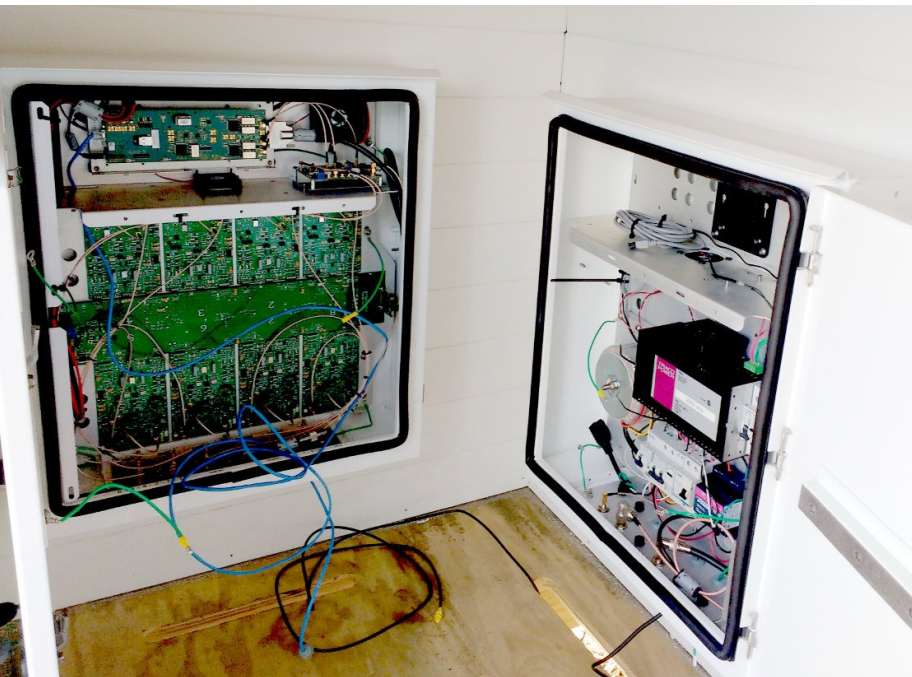


MK-III receiver engine (University of Hawaii)



University of Hawaii HFR (100 built):

- all-in-one, 24V solar/wind ready
- passively cooled, no A/C
- one 2.5" 4Tb drive = 4 years raw data
- all components outsourced
- mostly commercial off-the-shelf
- qty 40 cost about \$36,000



Processing HF Radar data for currents:

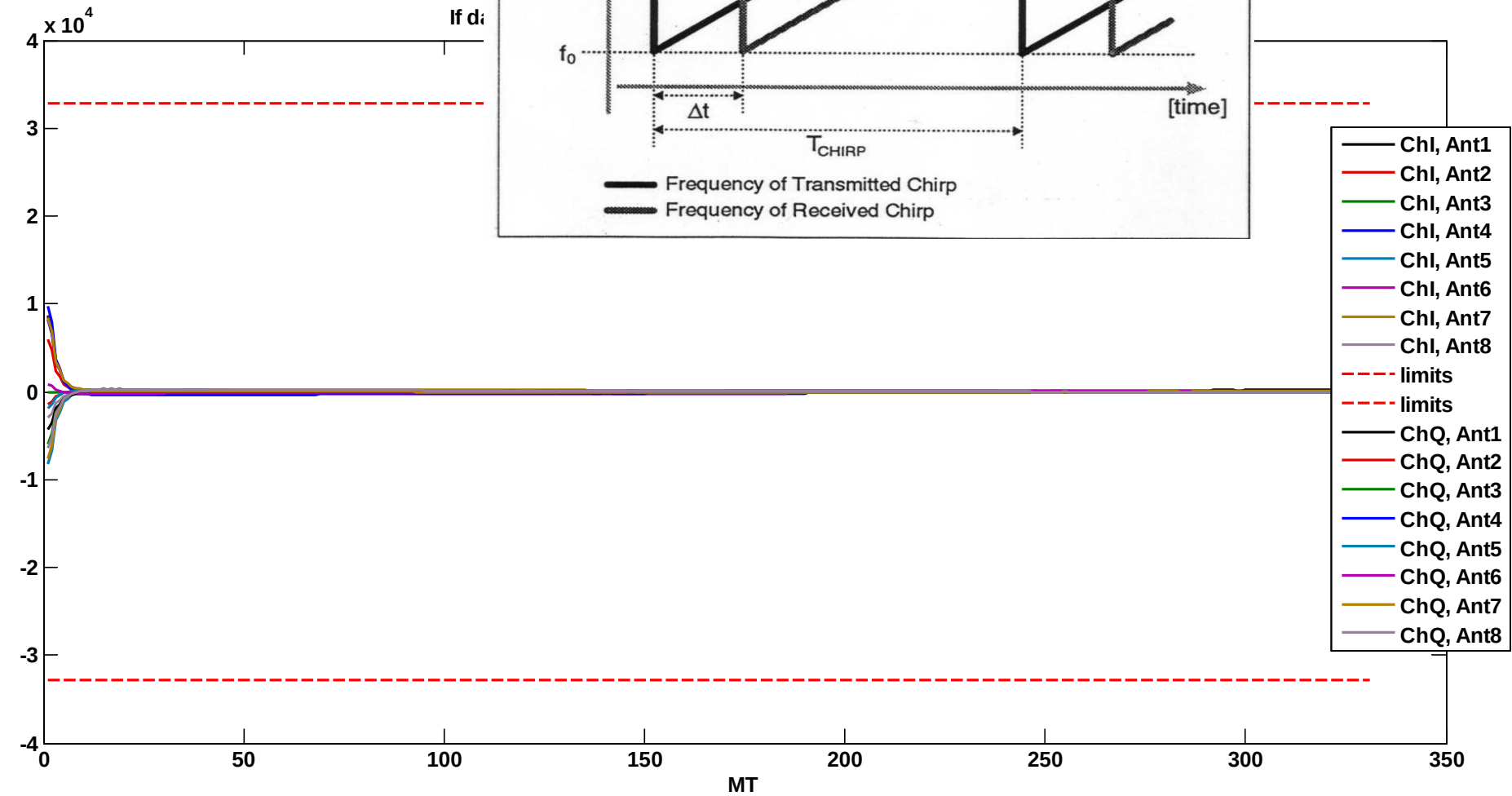
1. time series of digitized received antennas
2. range-resolving Fourier transform
3. Doppler-resolving Fourier transform
4. azimuth-resolving beam-forming transform
5. Doppler-shift tracking of Bragg echoes

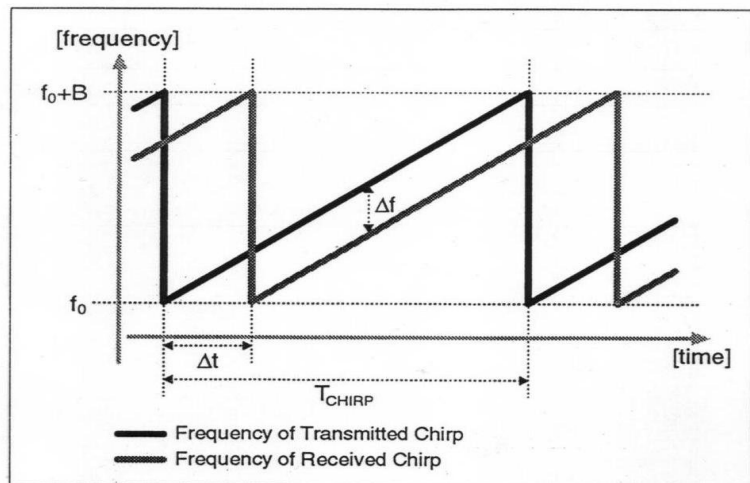
Kap

2016235004

0

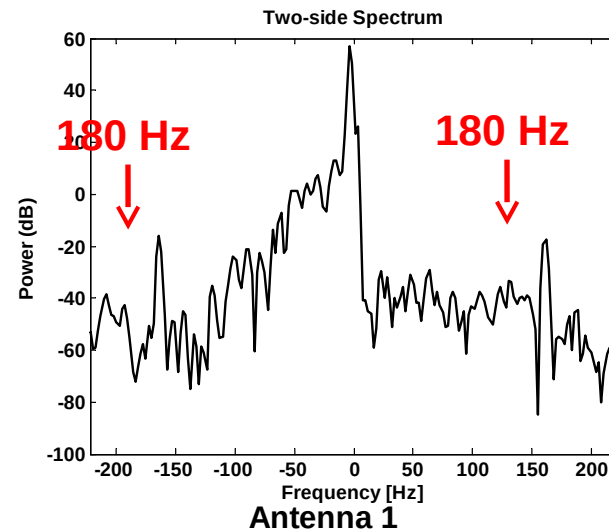
(22-Ago)



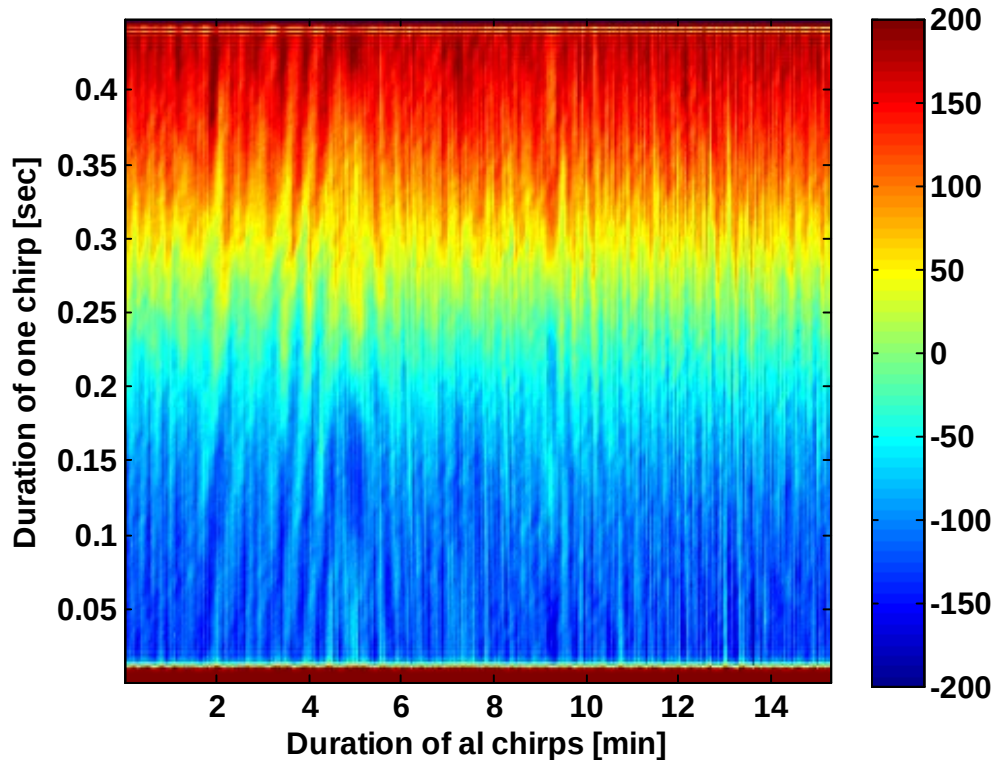


KAP

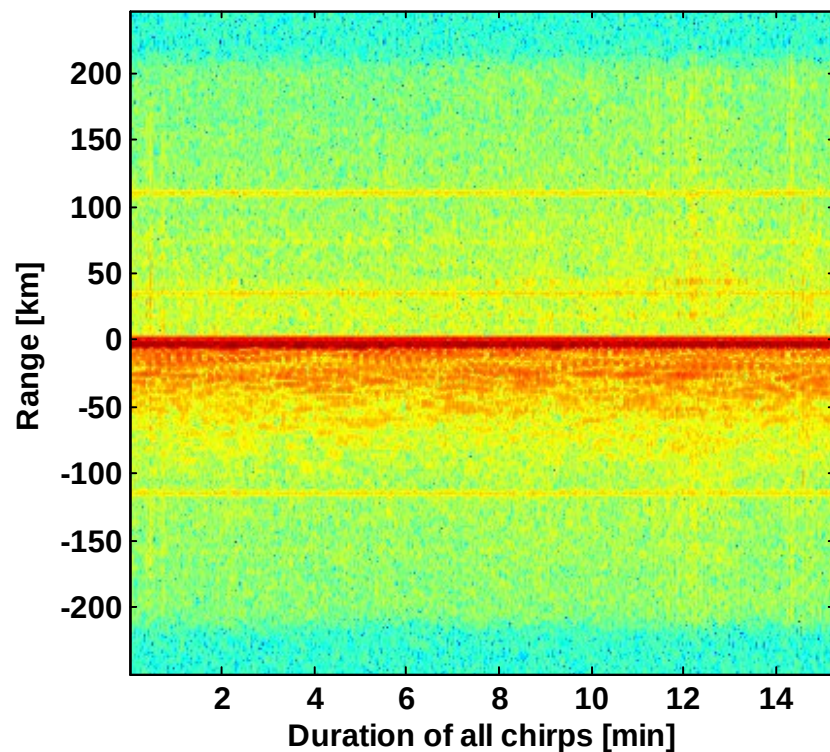
20162350040



Raw data; antenna 1, channel I



Time Series



Range-resolving FFT

KAP

20162350040

Doppler-resolving FFT and beamforming

Doppler-range spectrum; Direction 15°

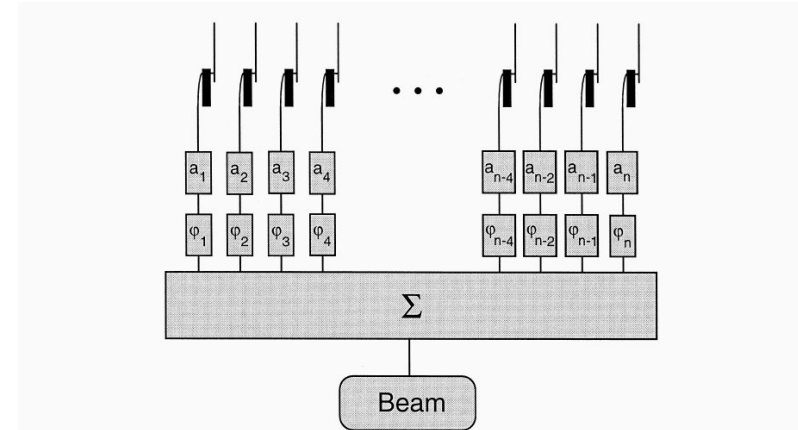
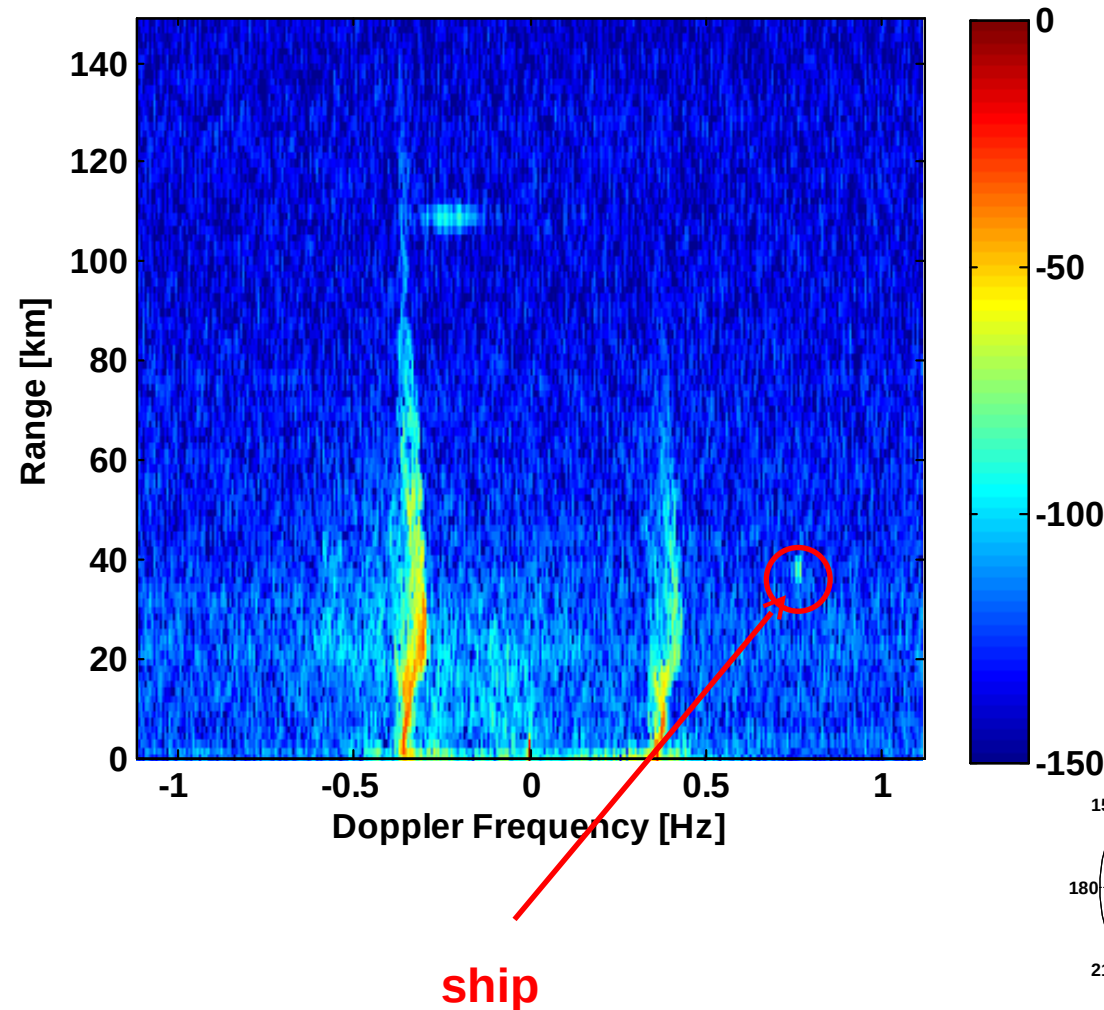
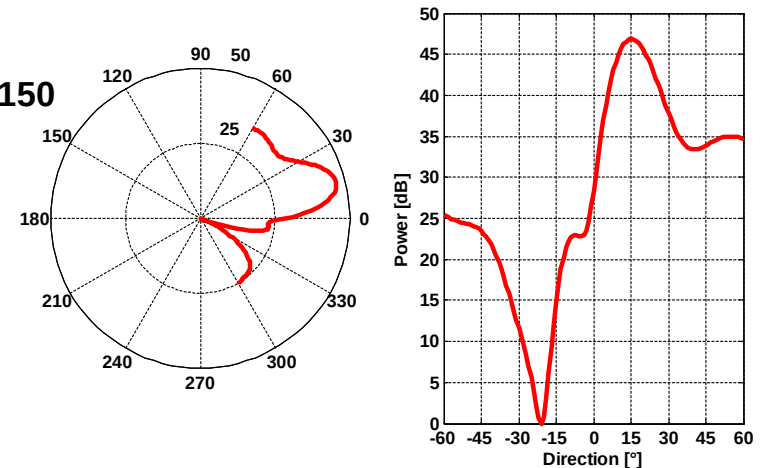


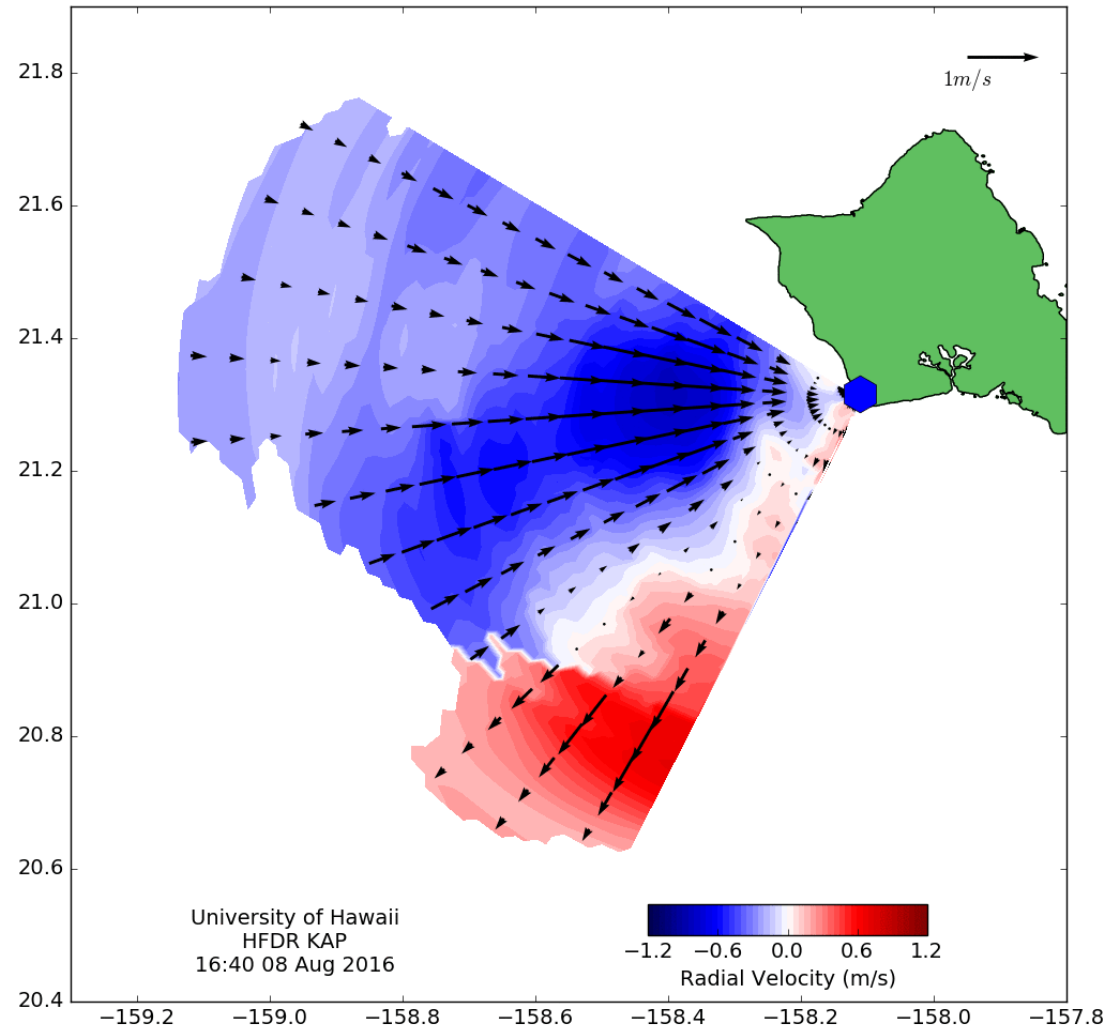
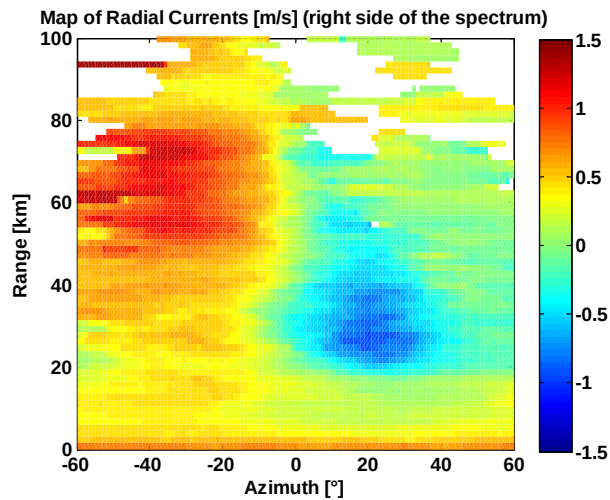
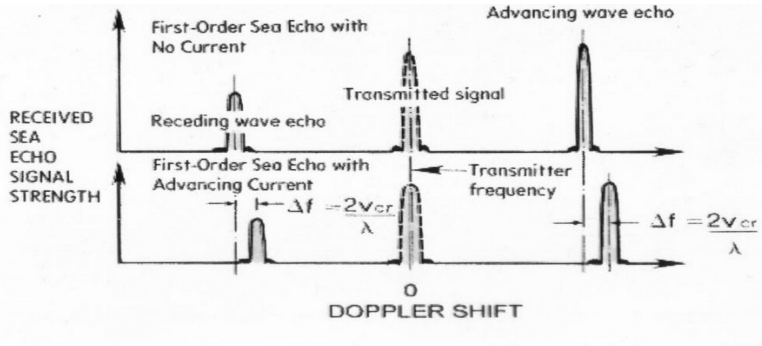
Fig. 10. Principle of beamforming. After weighing by a_i and phase shifting by φ_i the signals of n receive antennas are added.



KAP

Radial currents

20162350040



Low frequency flow in Panay Strait

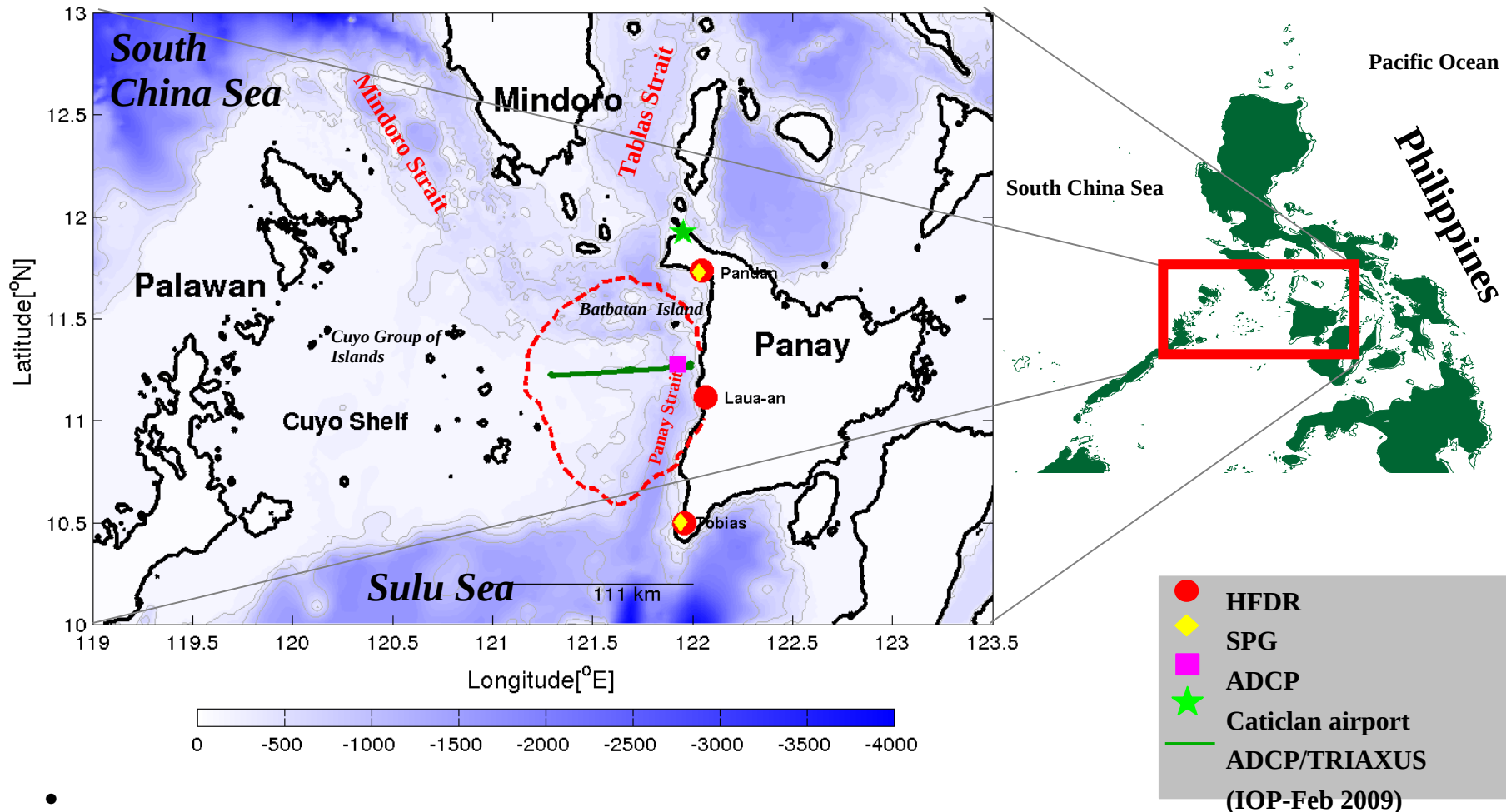
Ph.D. dissertation

Charina Repollo, U.P. Diliman

- characterize the dominant surface and subsurface flows
- assess the wind contribution on the onset and growth of cyclonic eddy
- describe the influence of eddy on biology

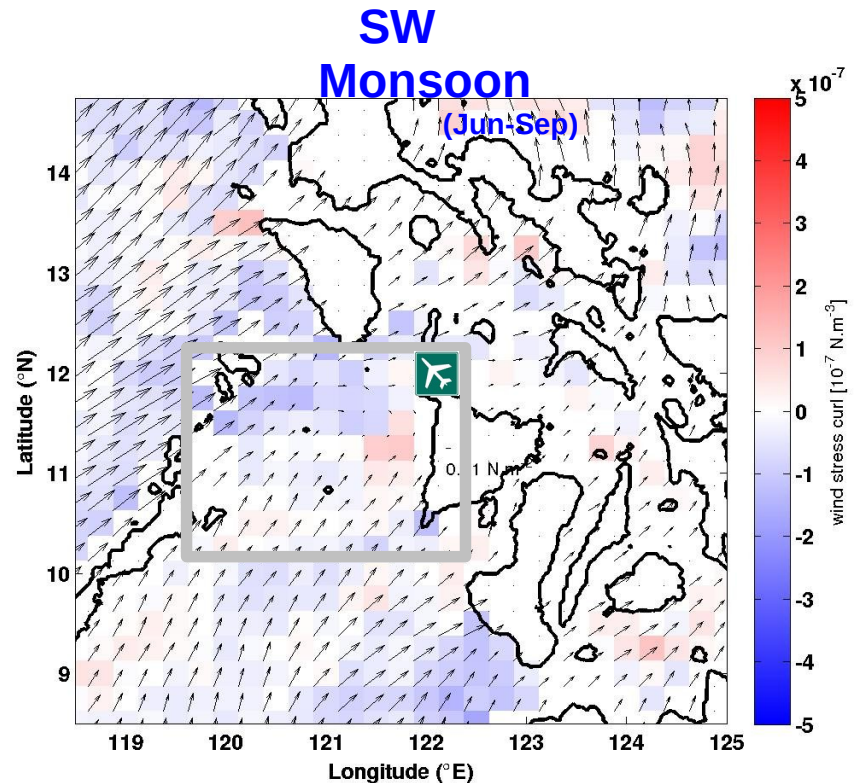
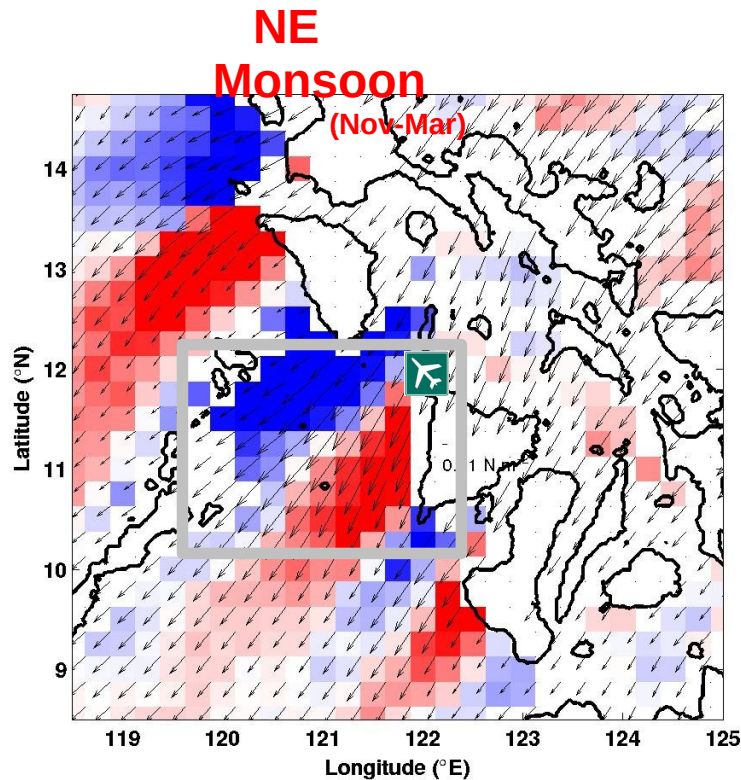
Philippine Straits Dynamics Experiment (2008)

Mindoro-Panay Strait: a branch of Indonesian Through-Flow



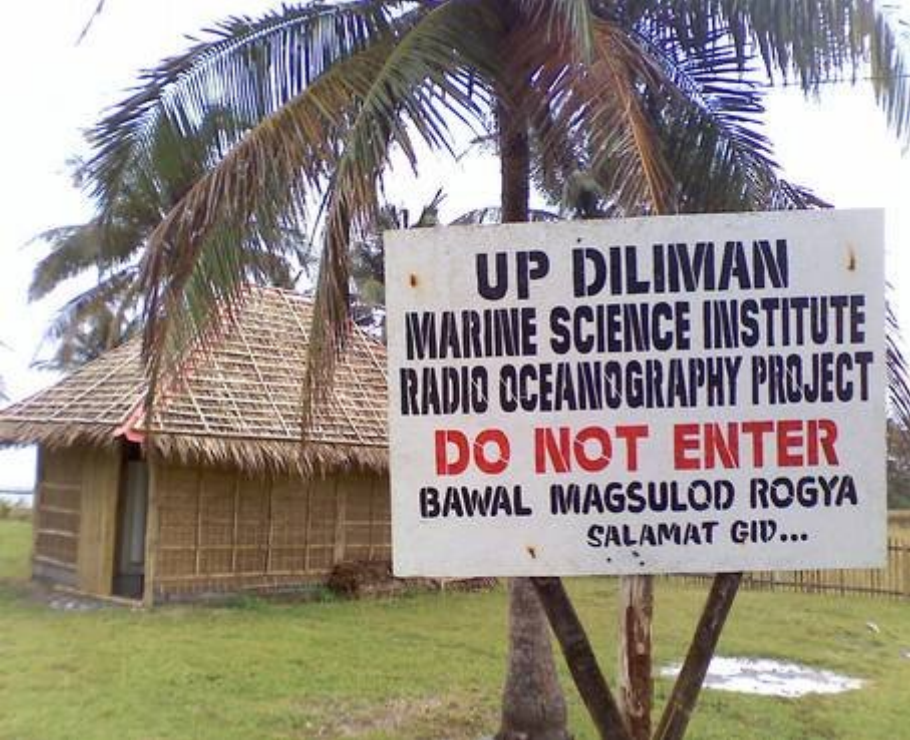
Wind stress and curl

(QuikSCAT satellite radar)

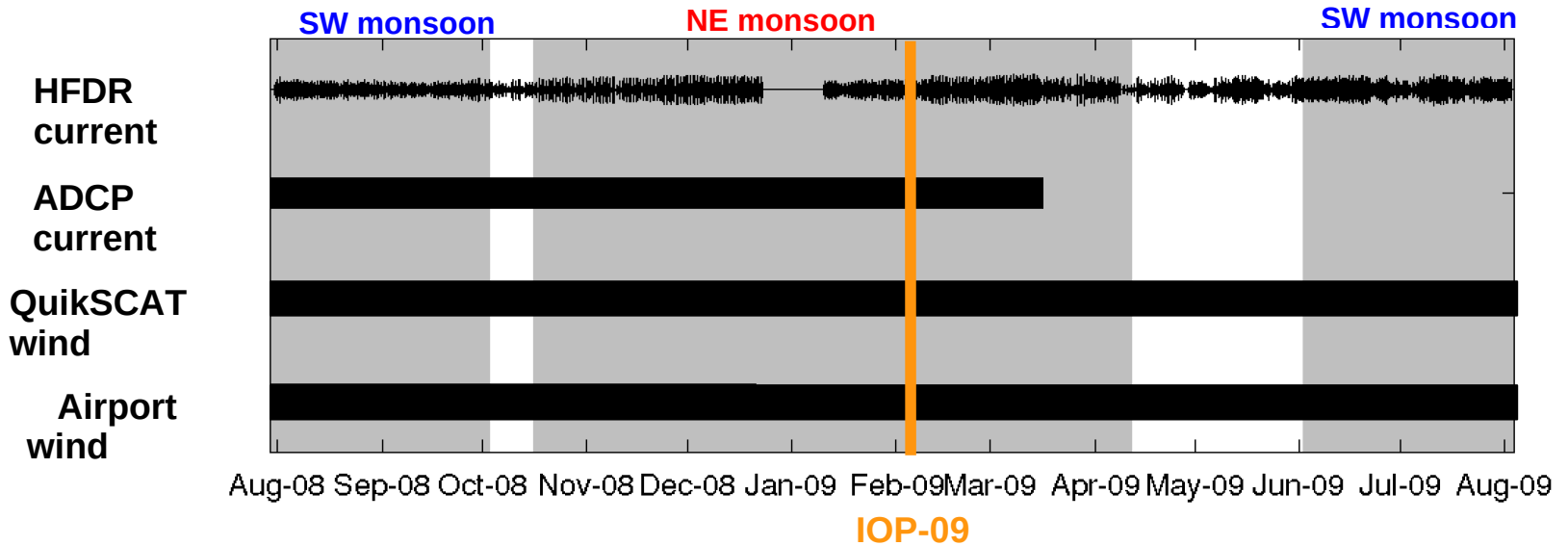


Pronounced seasonal cycle

- NE monsoon, strong wind stress curl in the lee of Panay Island
- SW monsoon, curl dipoles absent with random wind direction

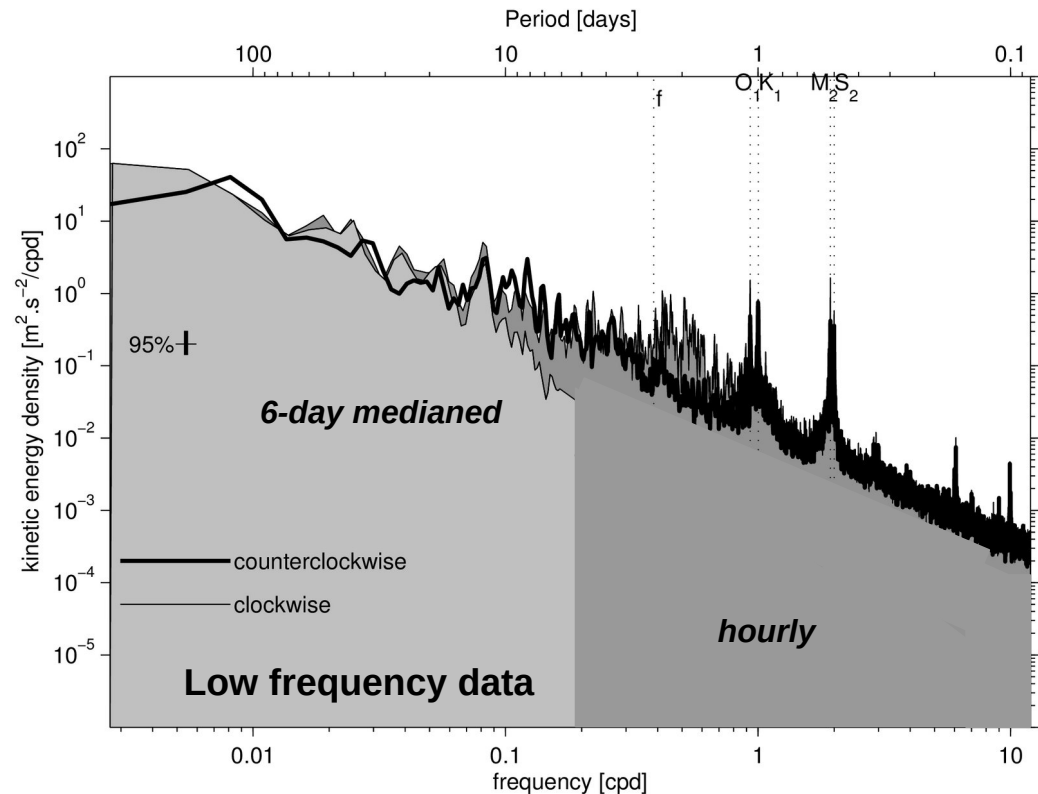


Data



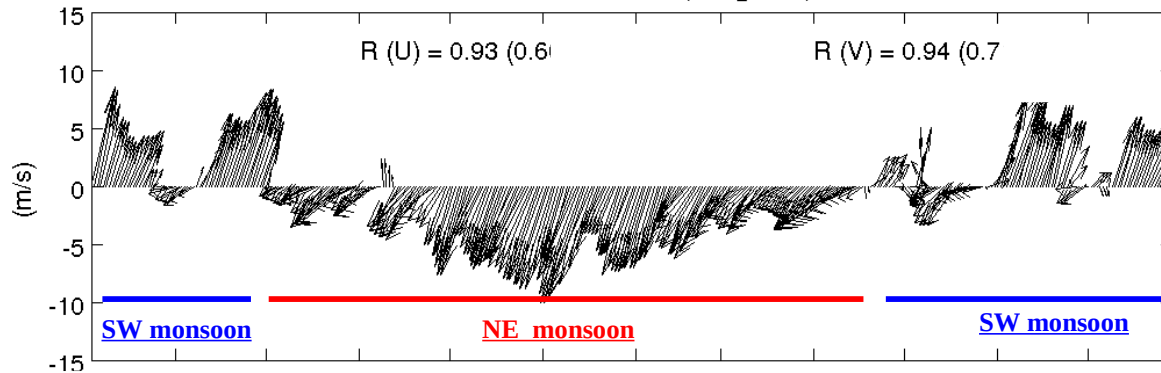
Low-frequency time series obtained by

- removing the tides (*t-tide*)
- 6-day running median

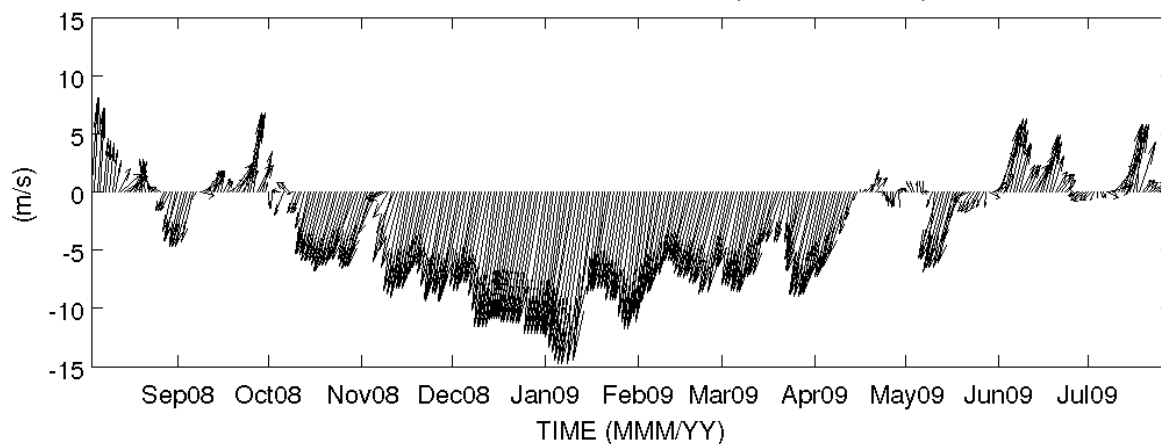


Local wind

observed wind (airport)

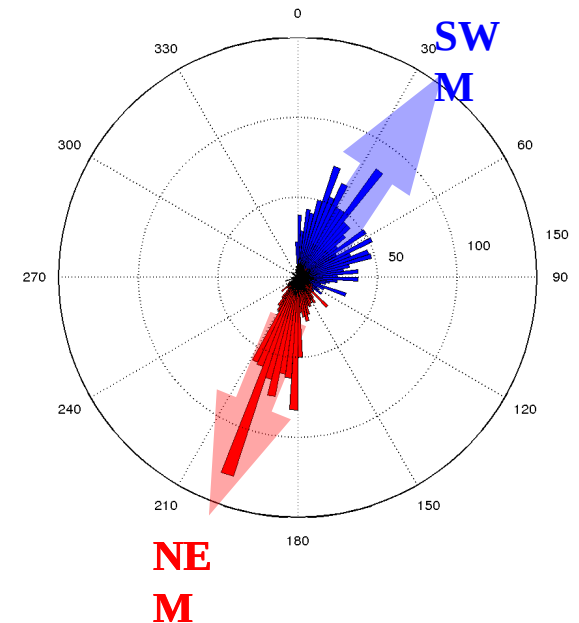
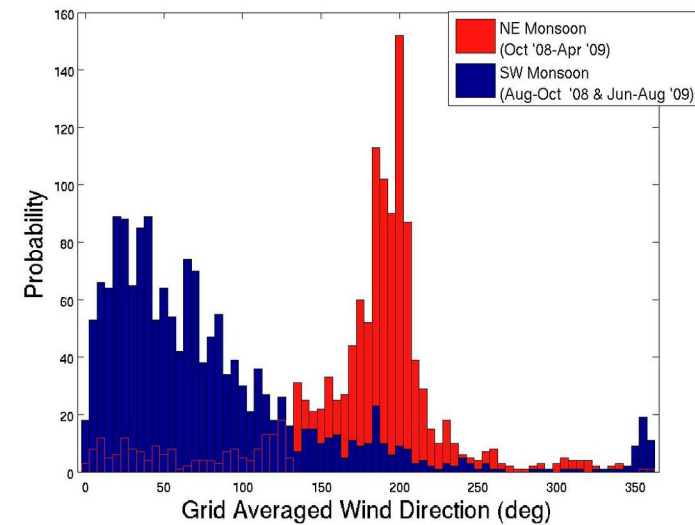


satellite-derived wind (QuikSCAT)

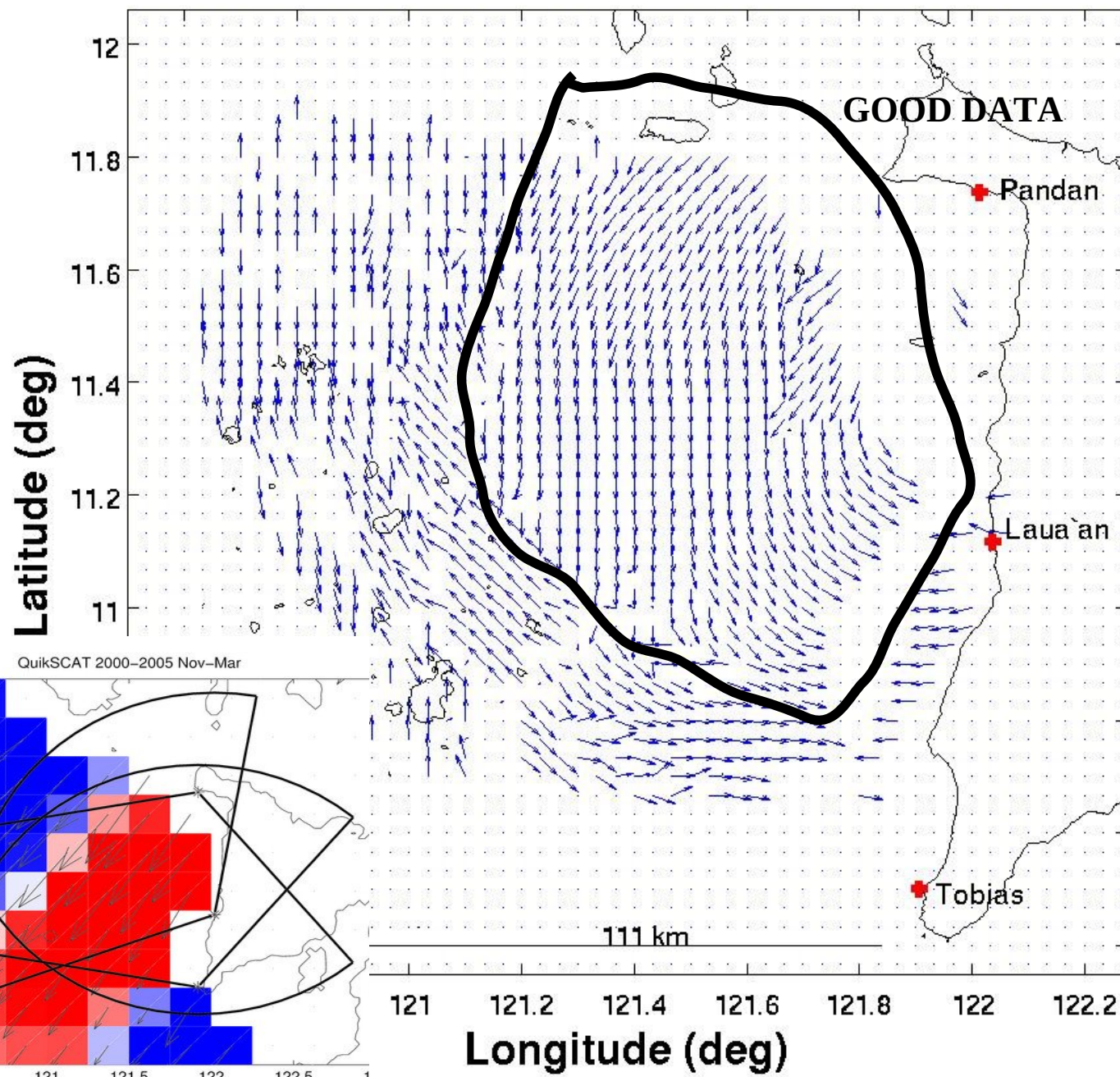


- Observed and satellite-derived winds well-correlated
- Persistent northeasterly wind Oct - April
- Variable southwesterly wind May - Sep
- Well-defined transition periods, October and April

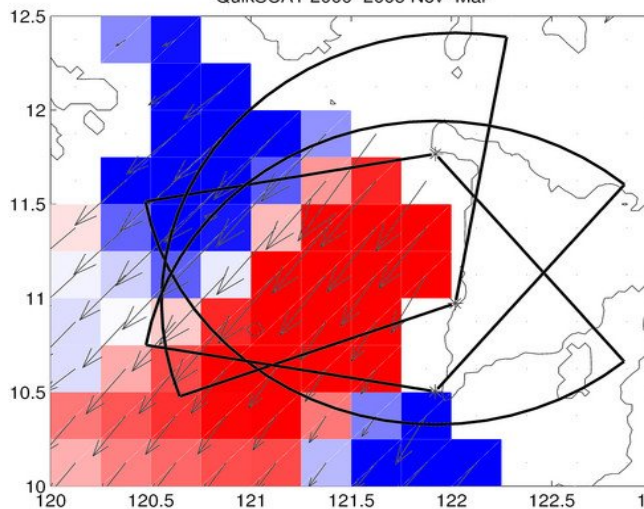
HFDR wind direction



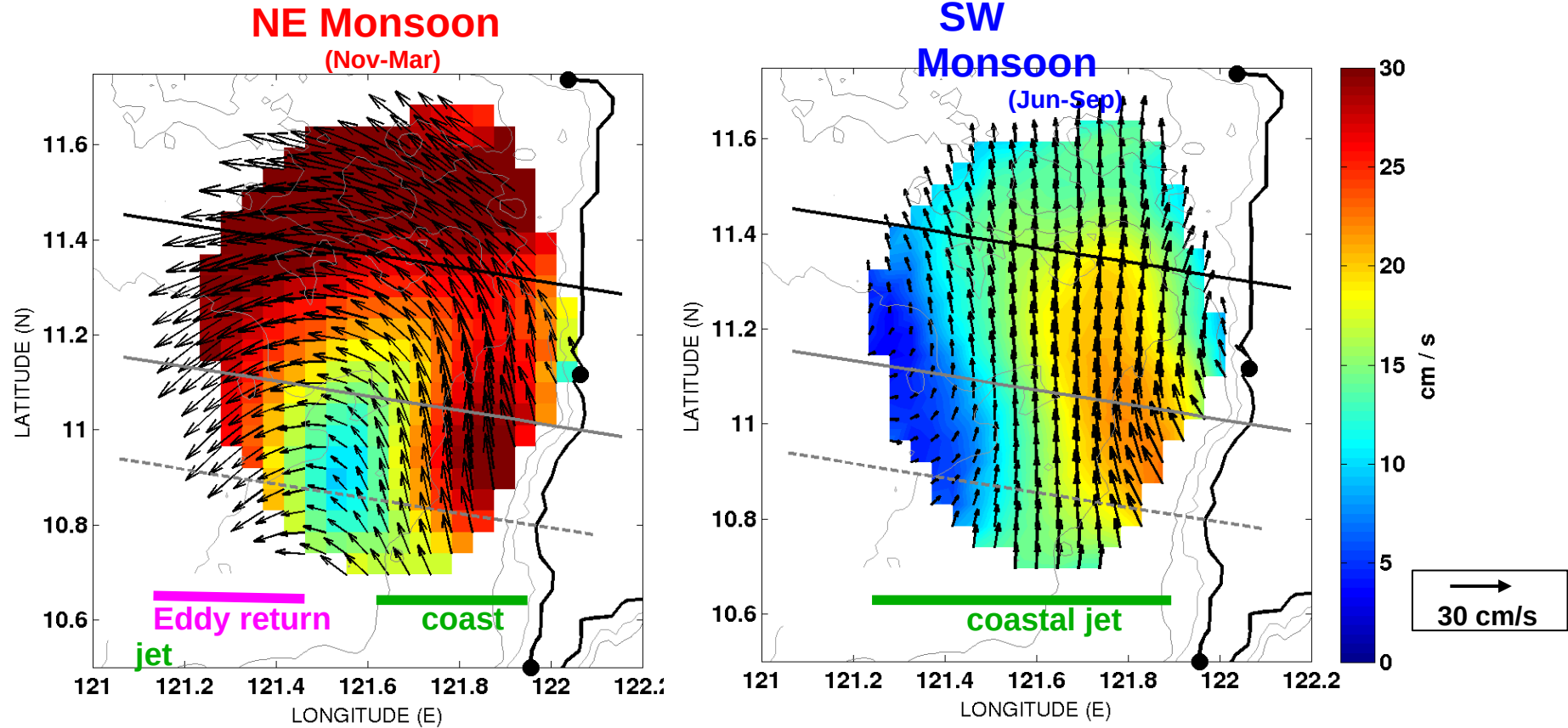
NE Monsoon



QuikSCAT 2000–2005 Nov–Mar

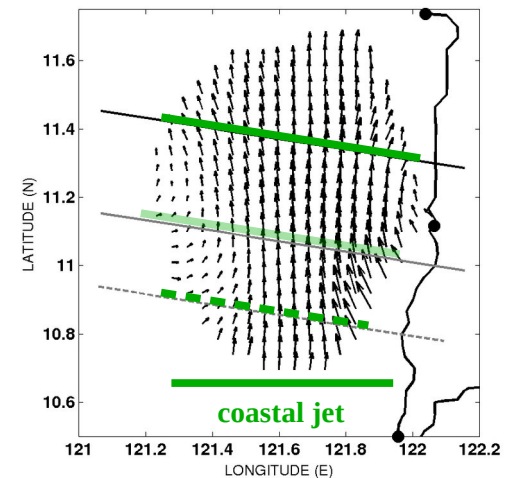
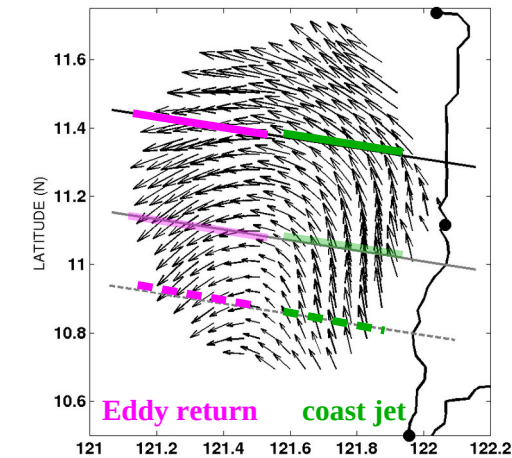
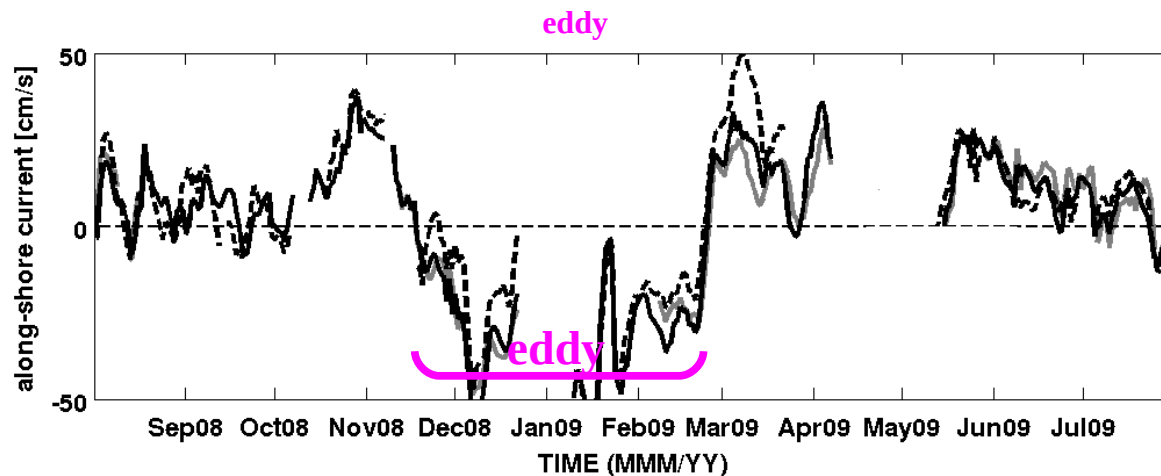
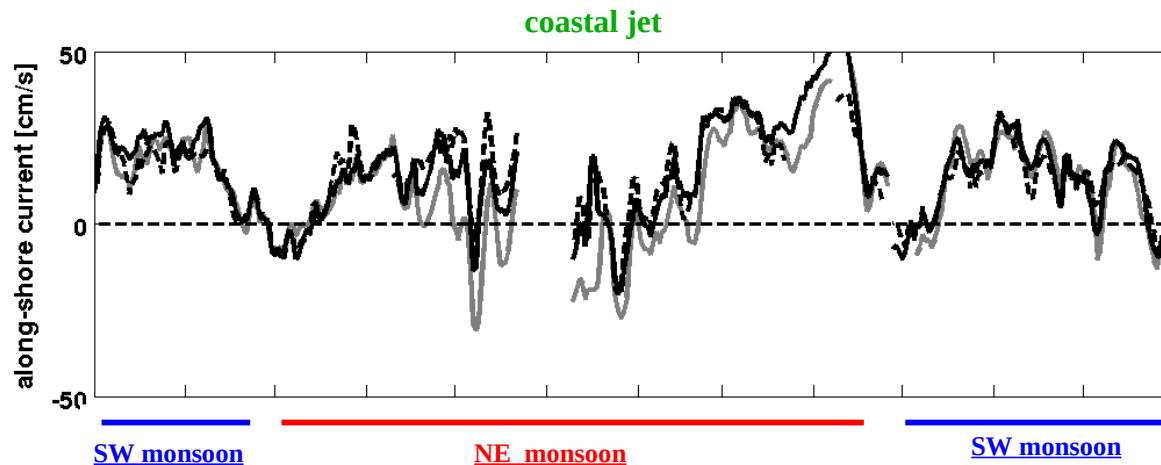


Surface flow (HFDR)



- coastal jet – northward alongshore flow from the coast to the center of the eddy
- eddy – southward return flow from the center of the eddy to the west

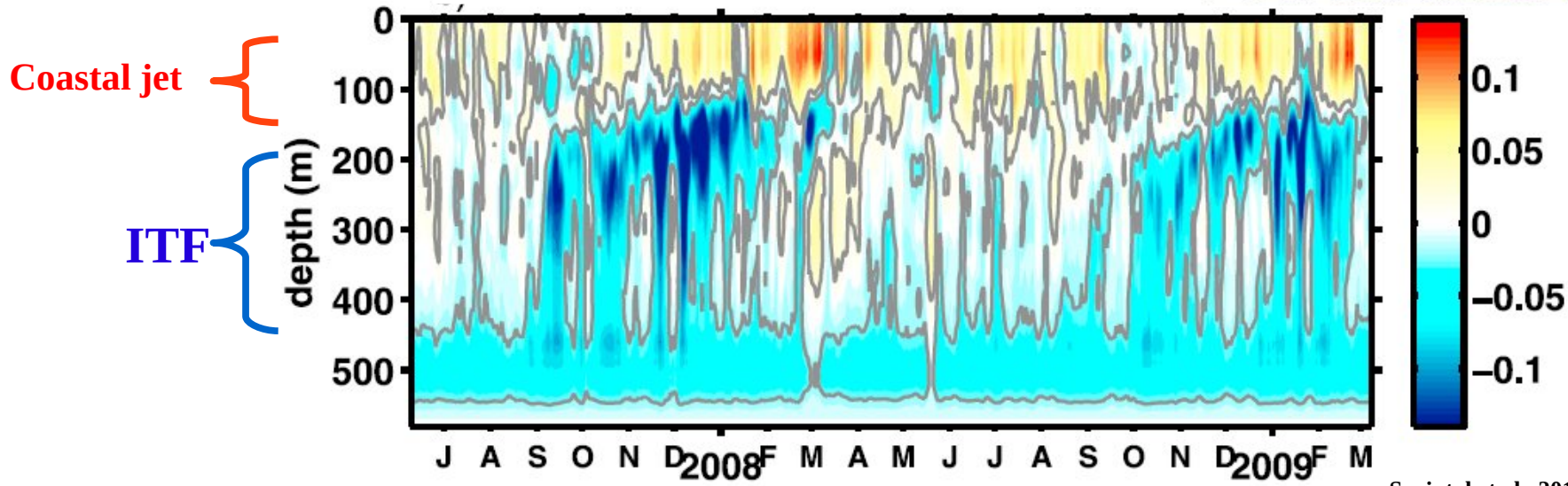
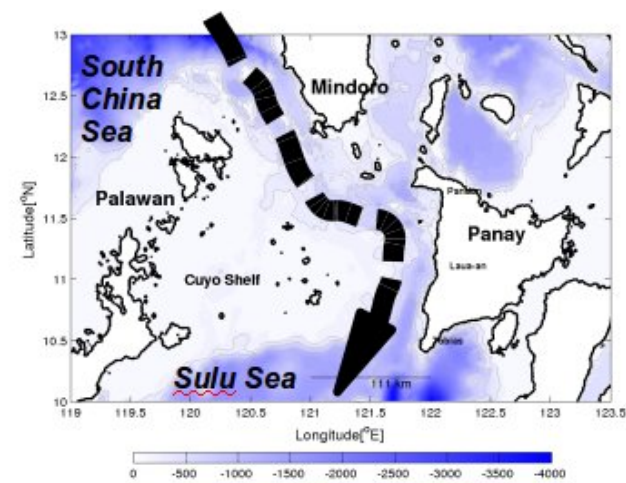
. Coastal jet and cyclonic eddy



- coastal jet is permanent
- cyclonic eddy is distinctly seasonal, NE monsoon
- well-defined transition periods, October and April
- intermittent variation of coastal jet concurrent with the eddy formation

- **Where is the Indonesian Through-Flow?**

(moves water from West Philippines Sea to Sulu Sea)



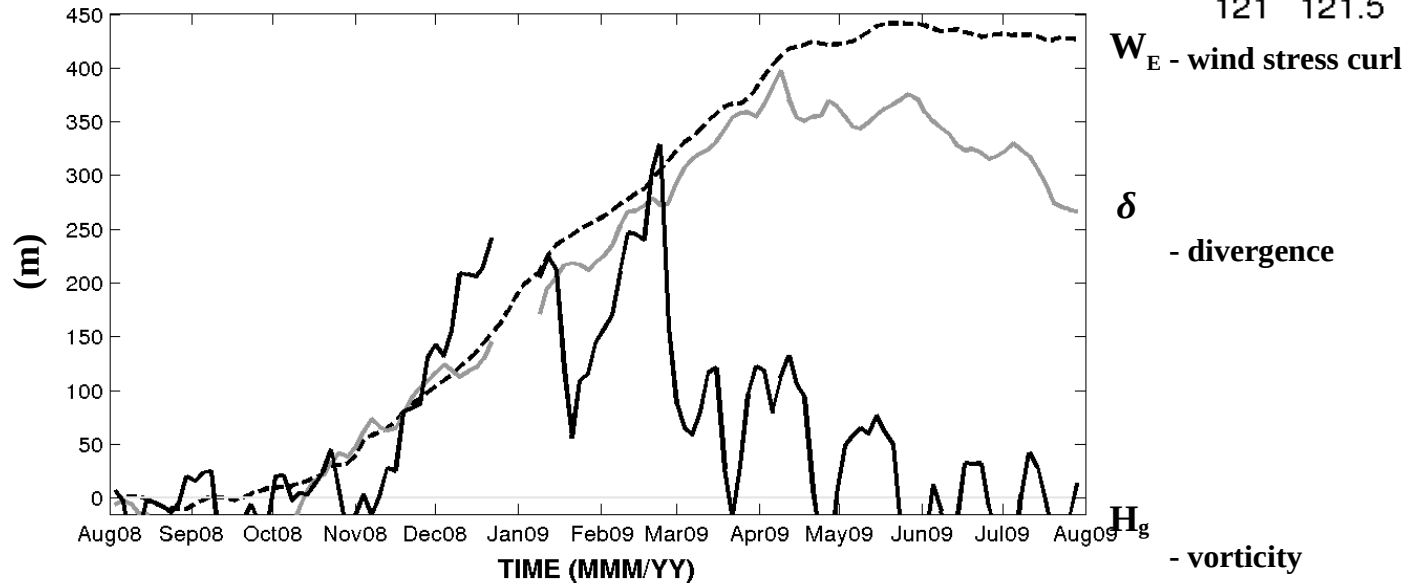
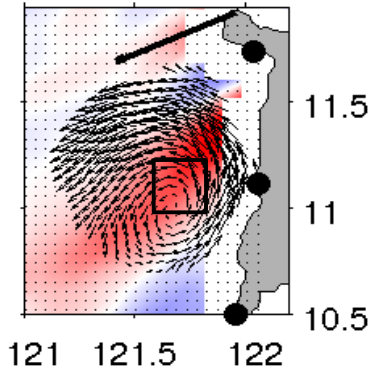
Sprintal et al., 2012

Vertical distribution of transport per unit depth (Sv m⁻¹) to Panay sill depth

- **Indonesian Through-Flow (ITF) is subsurface, under locally forced northward coastal jet**

• Time integral

Cumulative effect of wind stress curl generates divergence, permanently lifting the thermocline and increases vorticity



----- $\int_0^T W_E$ (COAMPS) W_E – Ekman pumping velocity

— $H_E \int_0^T \delta$ (HFDR) H_E – Ekman depth, best fit = 32 m

— H_g (HFDR) H_g – thermocline height

$$H_G = \frac{\zeta f L_G^2}{g'}$$

ζ - vorticity

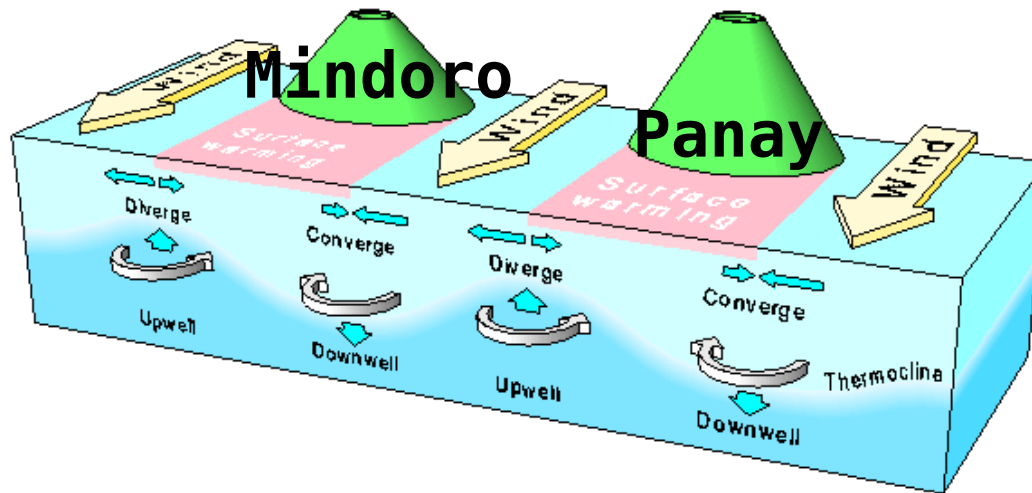
f - Coriolis parameter

L_G - radius the eddy, best fit=100km

g' - reduced gravity

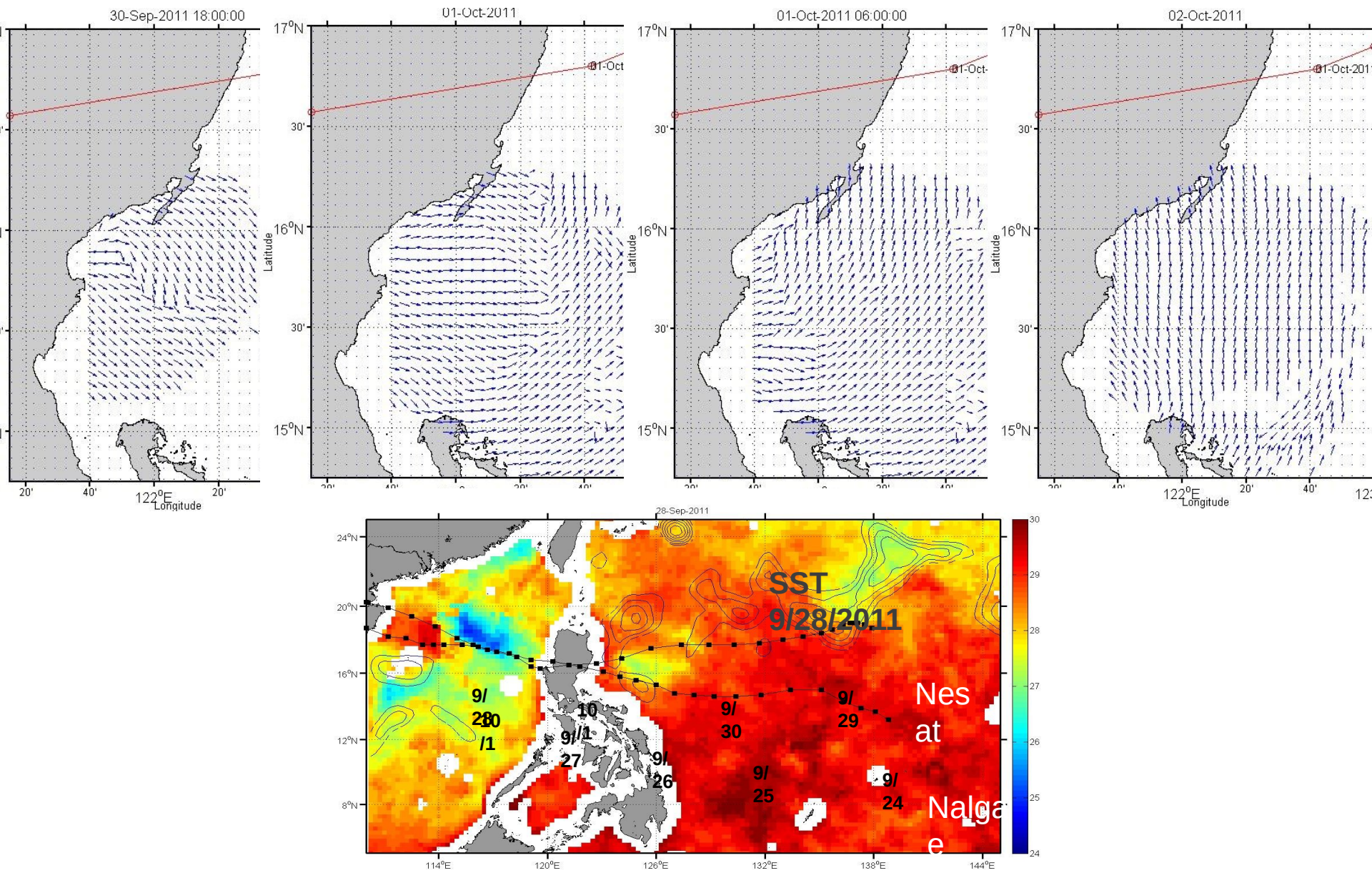
Conclusions

- Conceptual diagram showing Ekman pumping in the lee of islands
 1. wind intensifies between islands
 2. wind stress variations form positive wind stress curl in the lee of Panay
 3. induces divergent surface currents
 4. which in turn uplift thermocline
 5. pressure gradient spins-up eddy in geostrophic balance



- mechanism of cumulative wind stress curl to eddy kinetic energy

Wind direction from HFDR during typhoon passages (Ian Fernandez, UP-MSI)



Observations of the Luzon Strait through High-frequency Doppler Radar Scatterometers

Authors

Aiko Love B. del Rosario*, Charina Lyn Amedo-Repollo,
Cesar L. Villanoy
*adelrosario@msi.upd.edu.ph

Affiliations

Marine Science Institute, University of the Philippines-
Diliman, Quezon City, Philippines

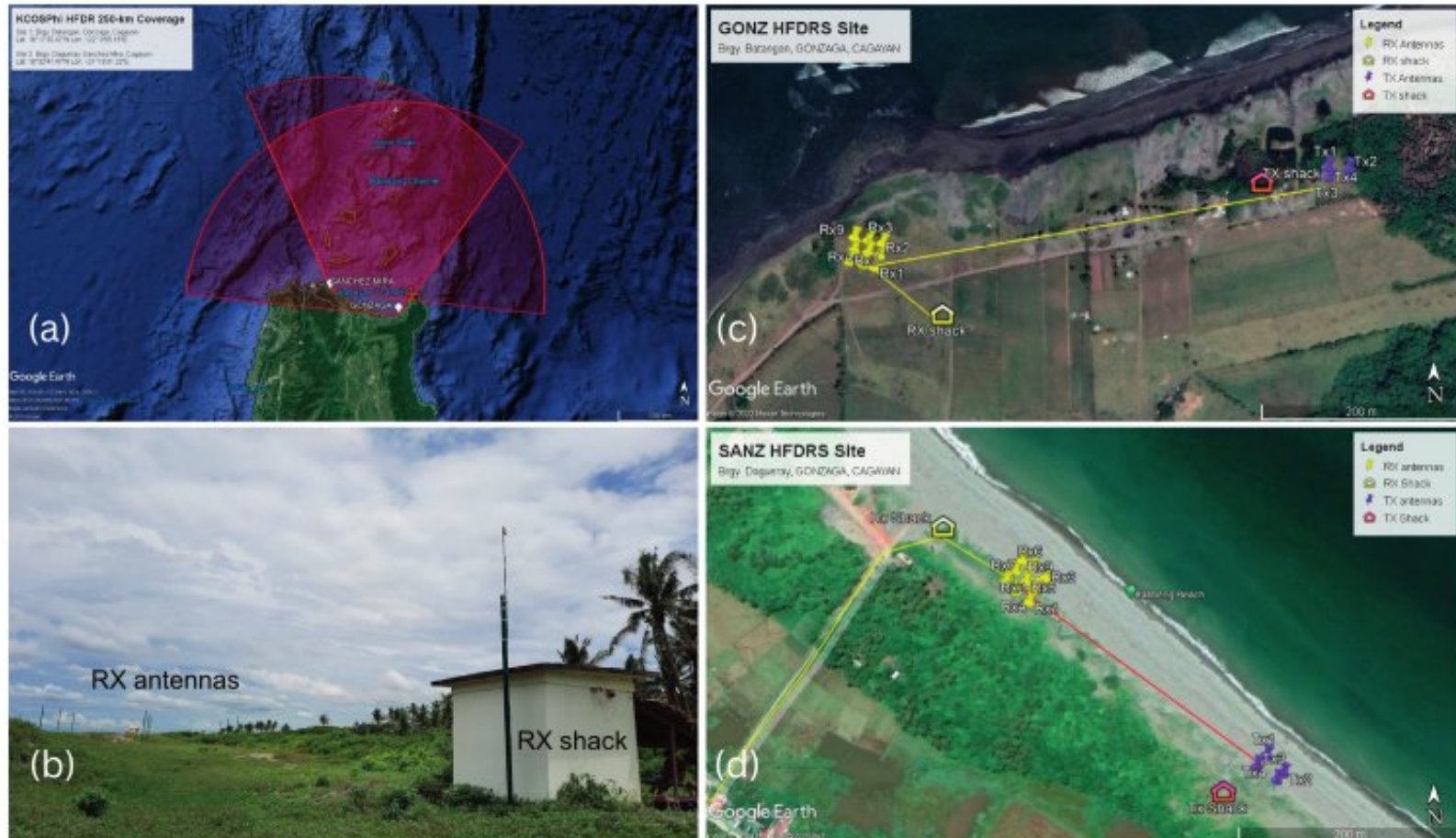
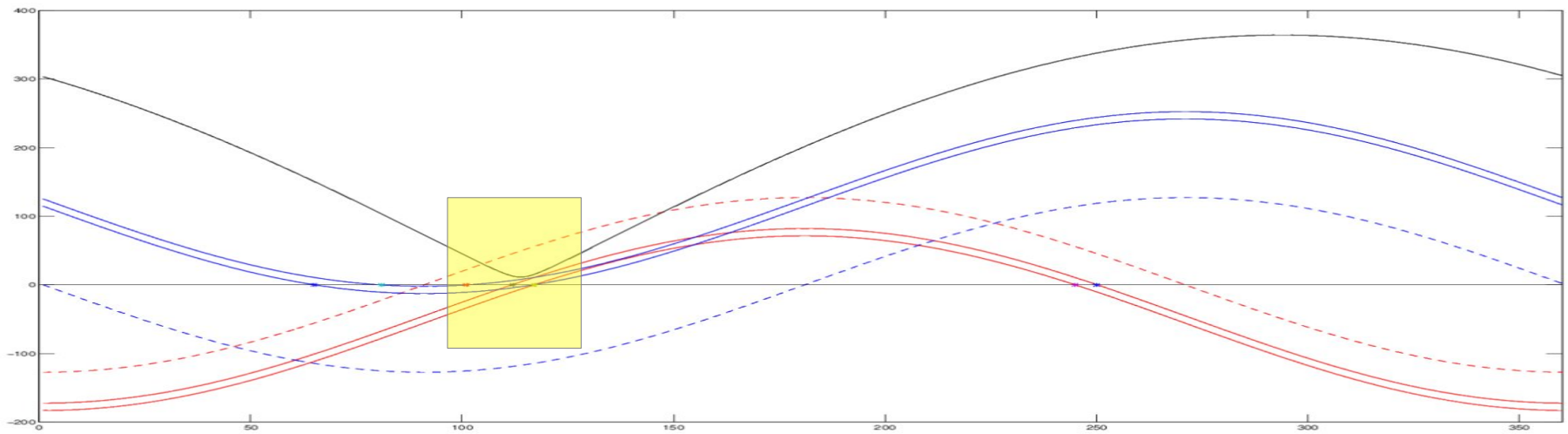
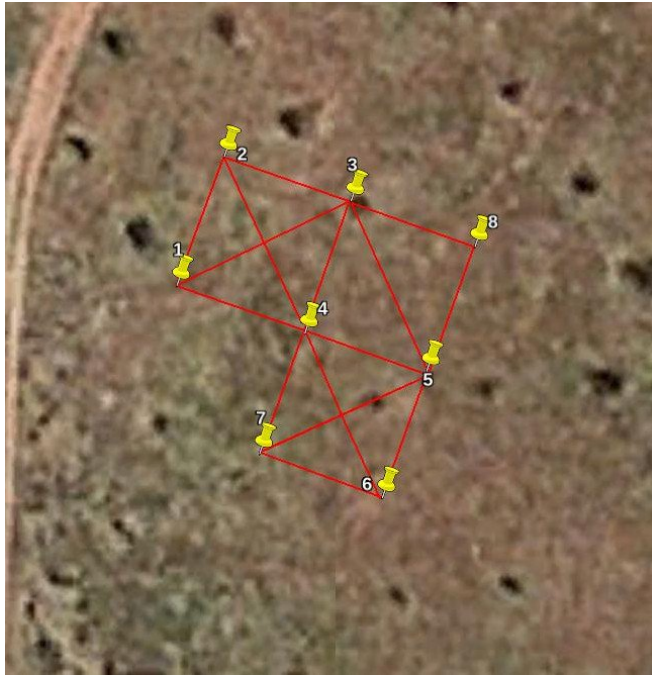
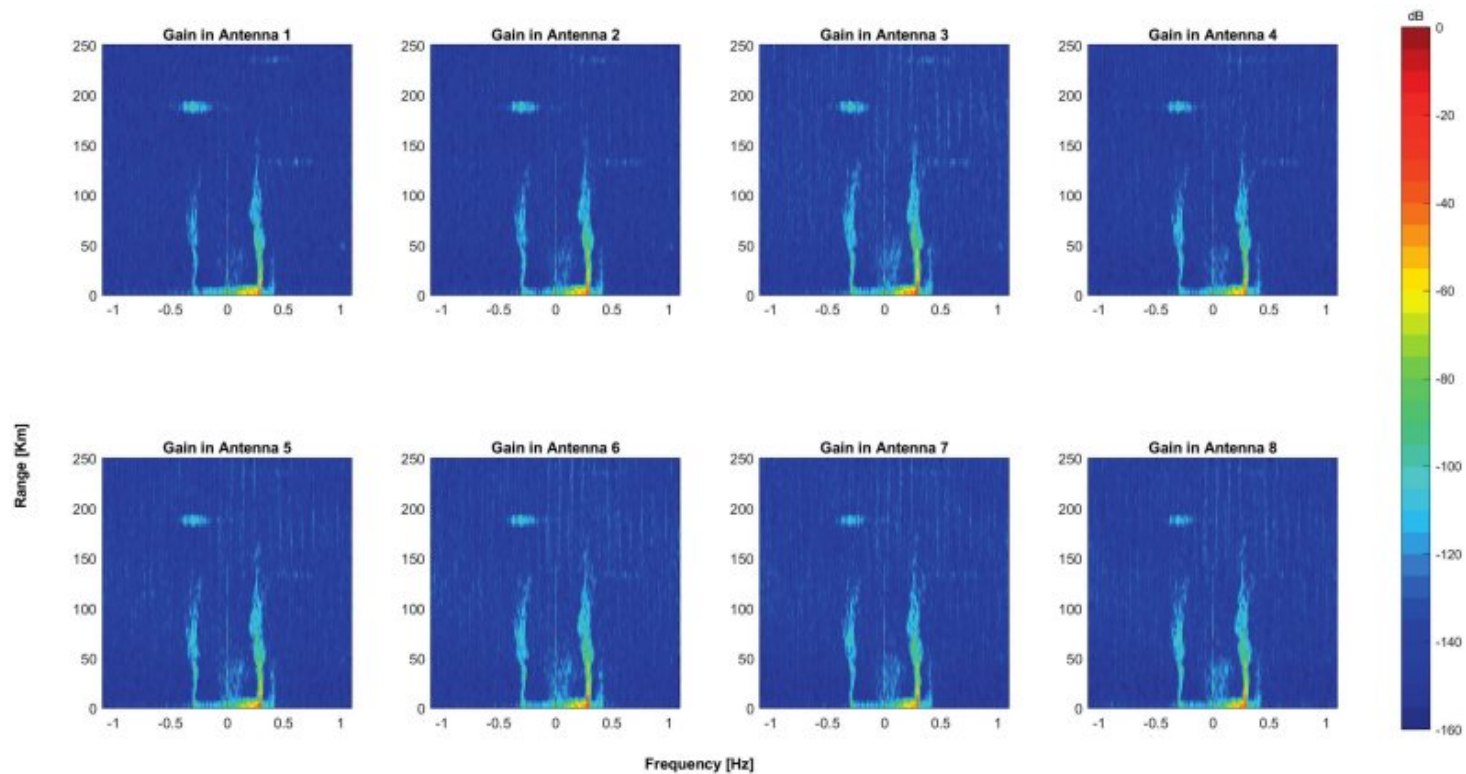


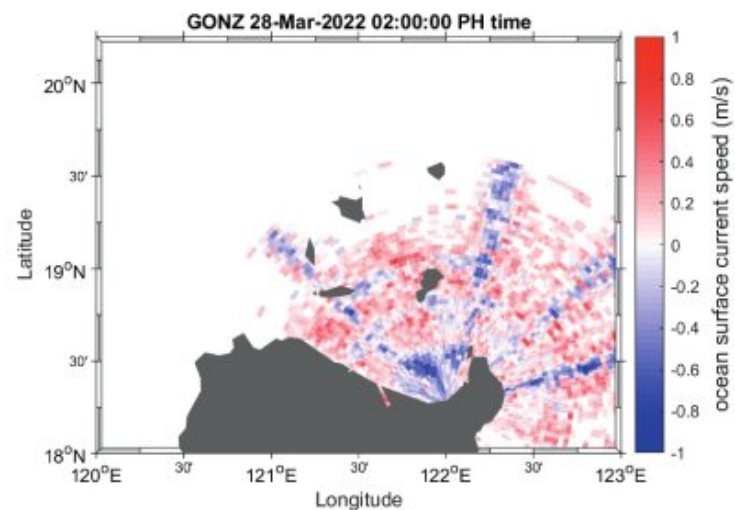
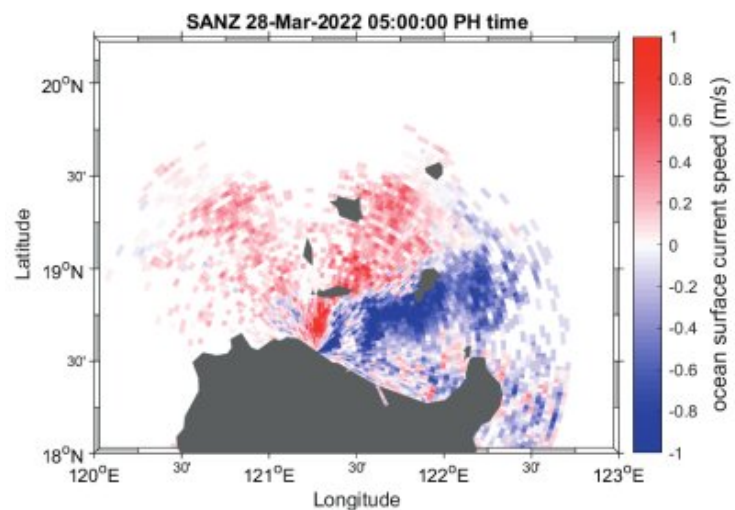
Figure 3. (a) Location of the two HF radar sites in Cagayan and the estimated coverage of the HF radar, (b) Set-up in SANZ site showing the RX shack and eight RX antennas, TX antennas not shown. Aerial view of the HF radar sites in (c) Gonzaga, Cagayan, and (d) Sanchez-Mira Cagayan

Novel array configuration: 3^2-1 grid for direction finding

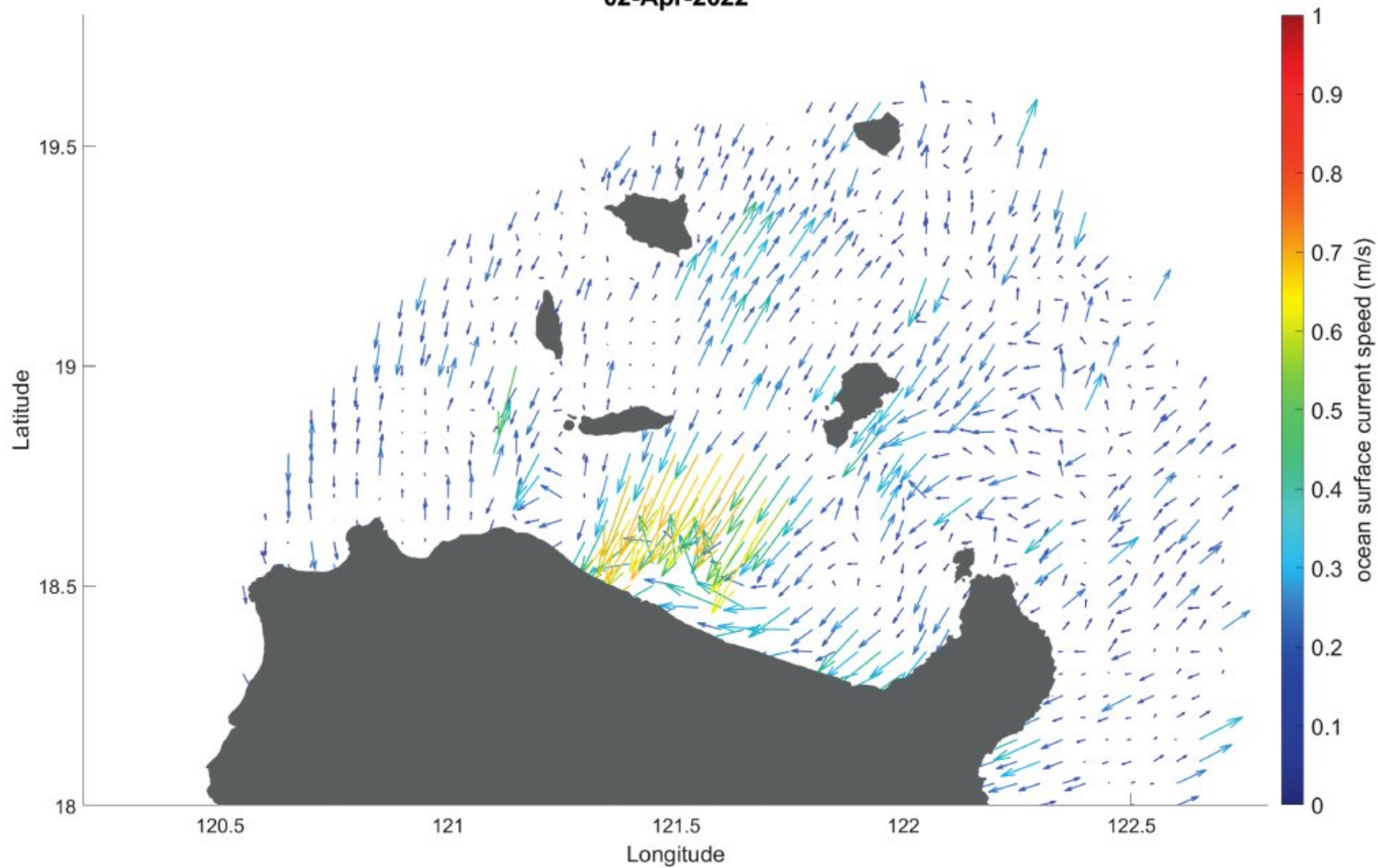




FILE: 20220910600_gonz.mat 01-Apr-2022 14:00:00



02-Apr-2022

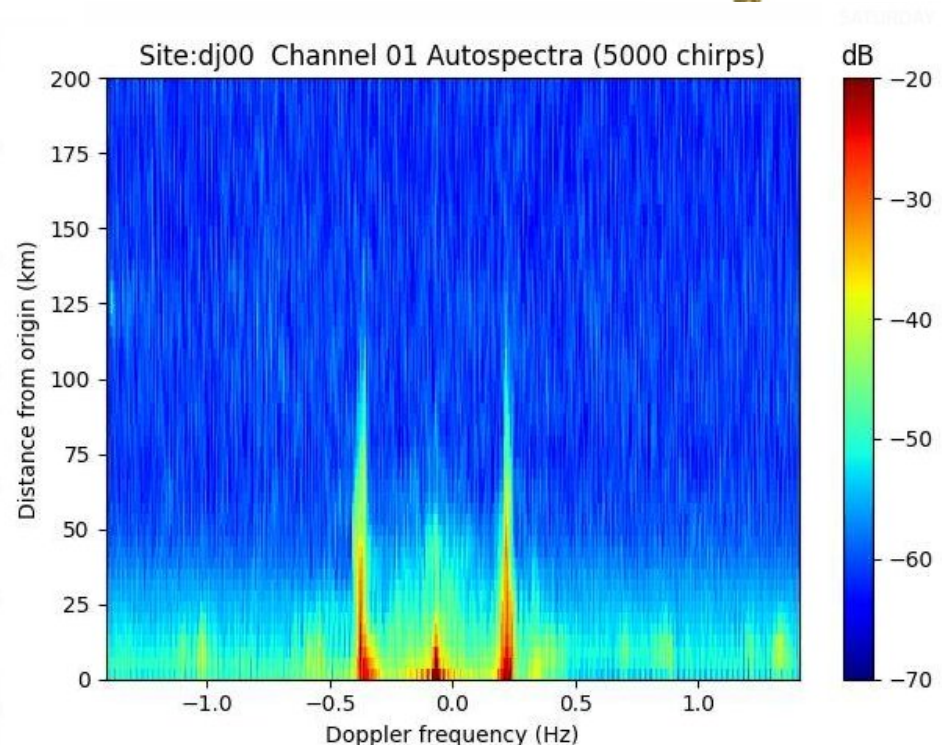


Recent development: all-constellations GNSS synchronization:

- use best PPS timing board on the market: U-Blox F9T
- tested ± 7 ns PPS jitter on fixed position
- firmware modules implemented in FPGA controller
 - ntp server on local network good to 1 ms
 - iterative clock-remapping of OCXO to 1 MHz using dedicated DDS by counting clock cycles between PPS
 - code to start chirp and ADC on exact PPS



- clock stability to 0.01 mHz maintained
by chip-scale Microsemi Rb clock
- *Applications:*
 - 1: distant TX and RX without cable connection
(allowing single-antenna TX)

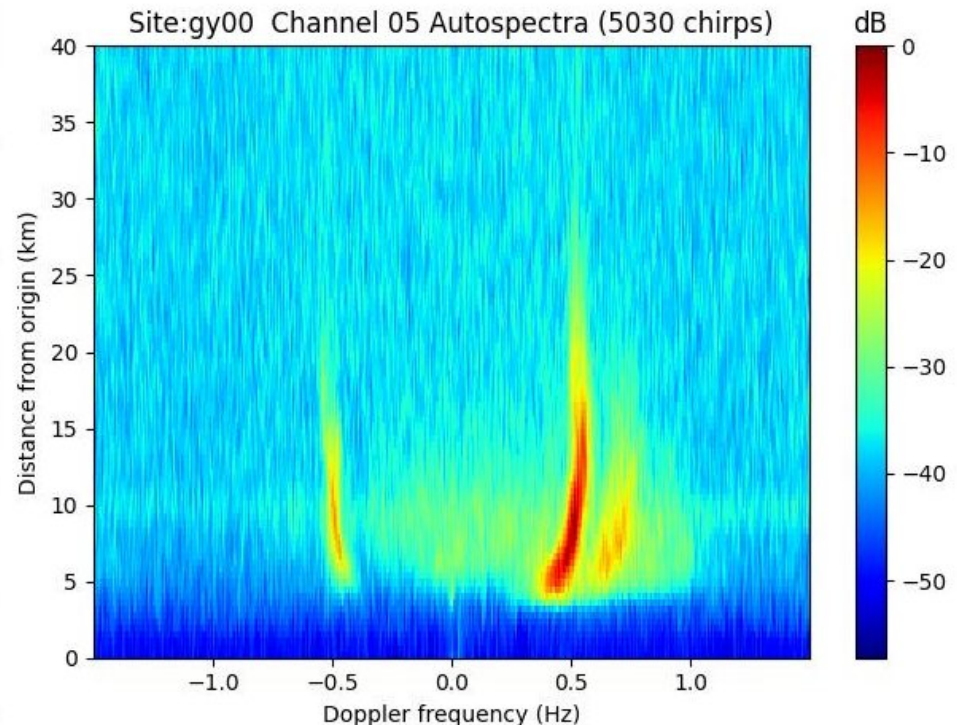


Recent development: all-constellations GNSS synchronization:

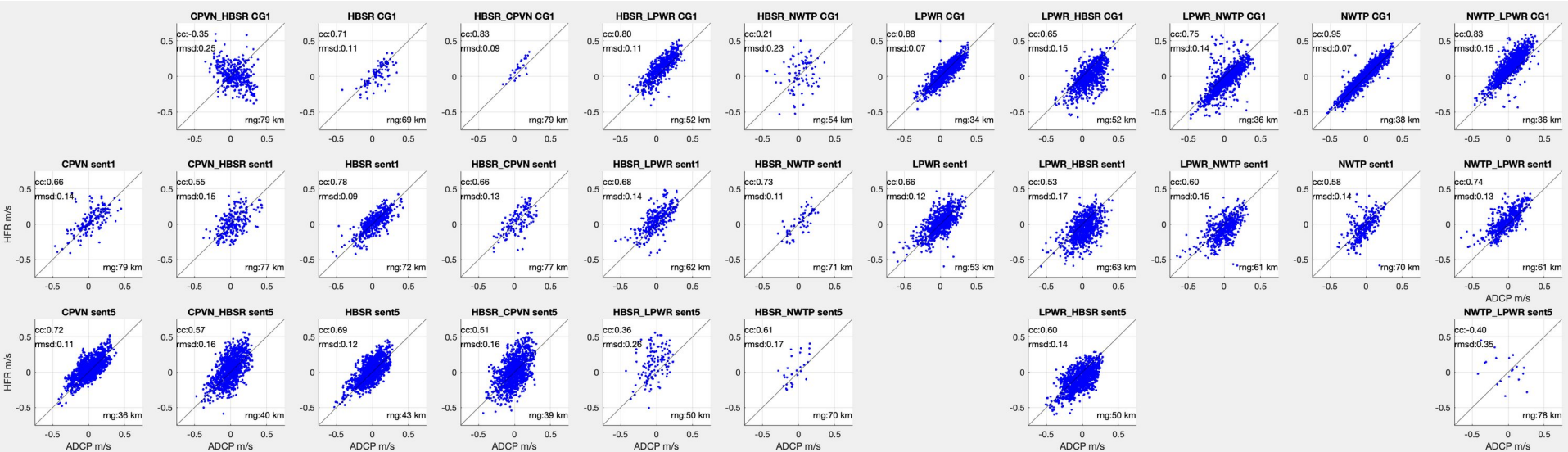
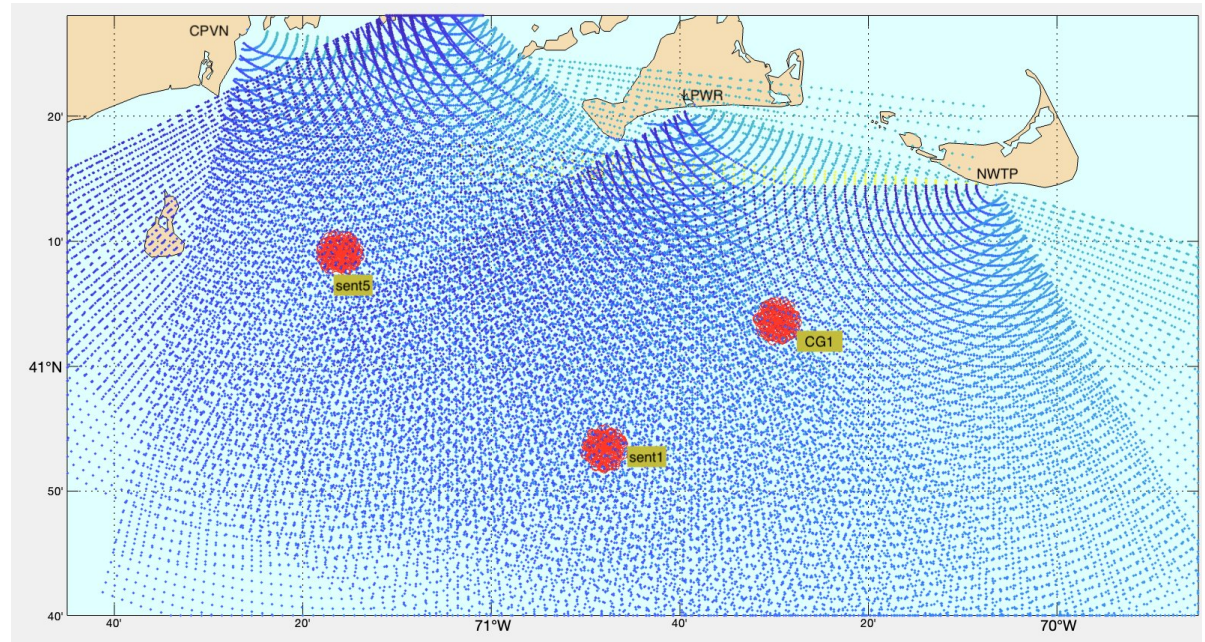
- use best PPS timing board on the market: U-Blox F9T
- tested ± 7 ns PPS jitter on fixed position
- firmware modules implemented in FPGA controller
 - ntp server on local network good to 1 ms
 - iterative clock-remapping of OCXO to 1 MHz using dedicated DDS by counting clock cycles between PPS
 - code to start chirp and ADC on exact PPS



- clock stability to 0.01 mHz maintained
by chip-scale Microsemi Rb clock
- *Applications:*
 - 2: multi-static operation for simultaneous elliptical and circular solutions (here: 8.5 km between TX and RX)



New England operational GNSS-synchronized multi-static array (LPWR/NWTP are atomic)



Space weather applications (ONR)

- use opportunistic well-known HFDR signal for ionospheric studies
- passive high-bandwidth receivers installed Palau, Taiwan, Philippines
- detect many chirping transmitters, few identified
- trend-setting paper by Scripps' group

Observations of Ionospheric Clutter at Near Equatorial High Frequency Radar Stations

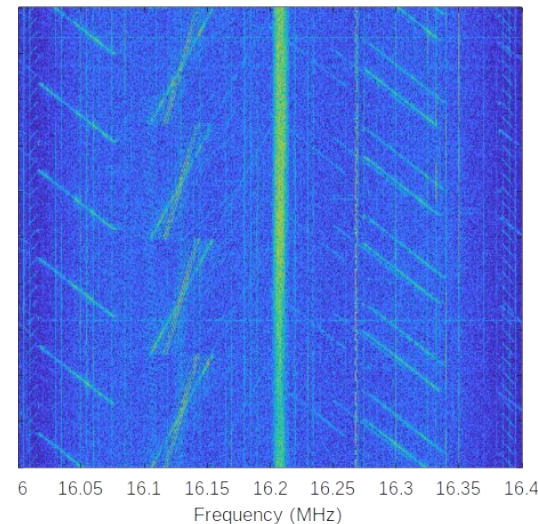
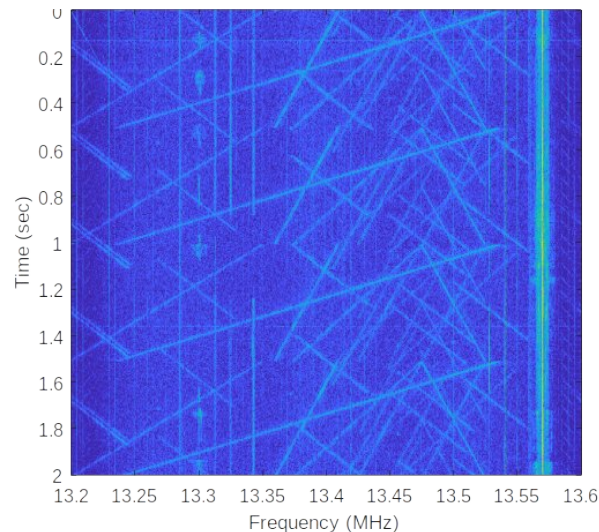
by Thomas M. Cook ^{*}†, Eric J. Terrill, Carlos Garcia-Moreno and Sophia T. Merrifield

Scripps Institution of Oceanography, University of California San Diego, La Jolla, CA 92039, USA

^{*} Author to whom correspondence should be addressed.

[†] Current Address: Ocean Modeling Laboratory, SRI International, Ann Arbor, MI 48105, USA.

Remote Sens. **2023**, *15*(3), 603; <https://doi.org/10.3390/rs15030603>



**Deployable Vector Sensor
Antenna Array**

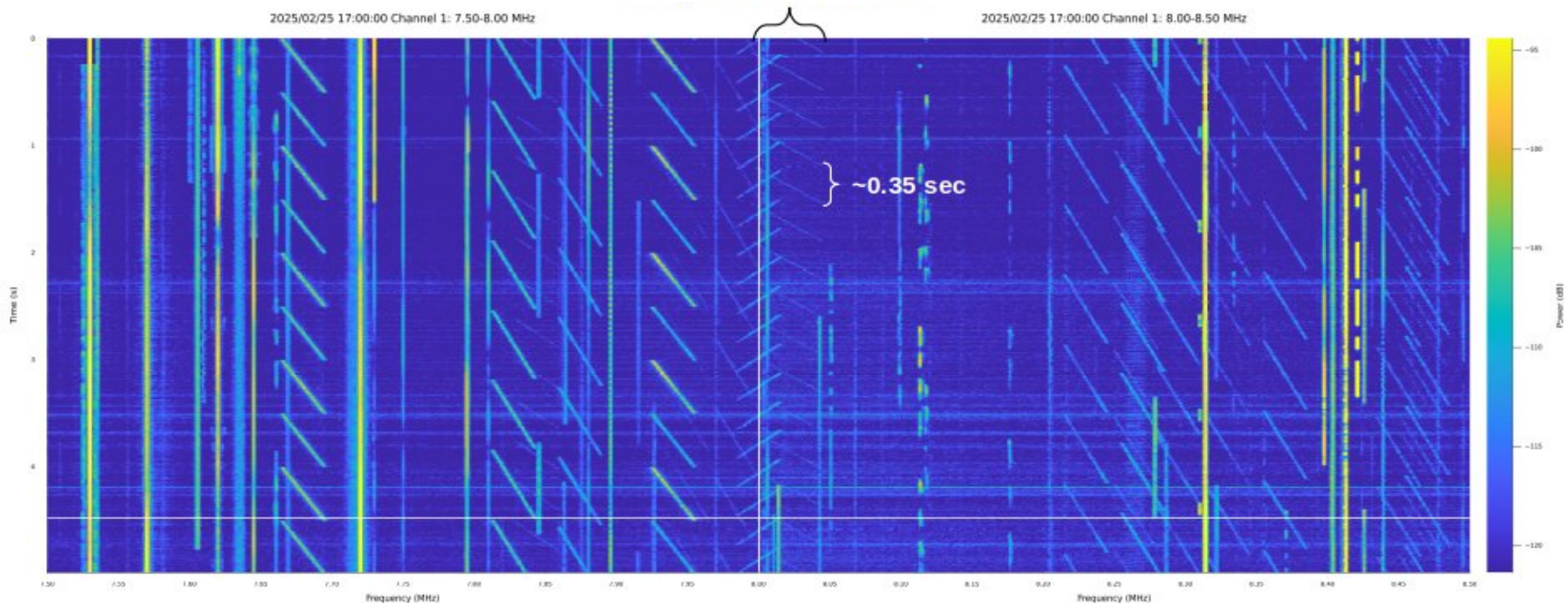
Space weather applications (ONR)

- use opportunistic well-known HFDR signal for ionospheric studies
- passive high-bandwidth receivers installed Palau, Taiwan, Philippines
- detect many chirping transmitters, few identified



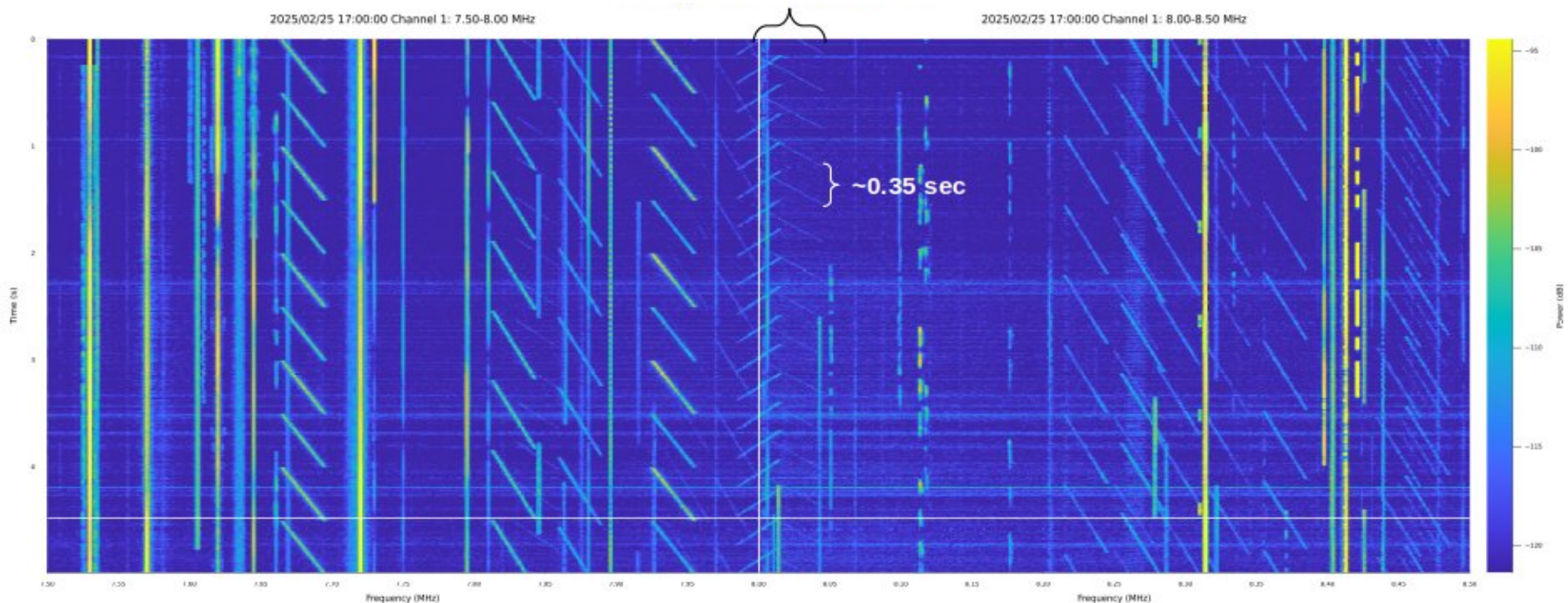
**Deployable Vector Sensor
Antenna Array**

MIT Lincoln Lab's MODI receiver on Palau:



Future developments:

- are we seeing the end of *homodyne* HF radars?
- are software-defined HF radars next?
- potential for using opportunistic well-known HFDR signals for transmitter-less multi-frequency passive receiver radars



ROW 2001**ROW 2002****ROW 2003****ROW 2004****ROW 2005****ROW 2006****ROW 2007**

ROW 2008

ROW 2009

ROW 2010**ROW 2012****ORCA 2014****ROW 2014**

ROW 2015

ORCA 2016

ROW 2017

ORCA 2018

ROW 2019

[Main](#) /

Radiowave Oceanography Workshops

The [University of Hawaii Radio Oceanography Laboratory](#) maintains archives of the presentations made at the Radio Oceanography Workshops ("ROW") and the Ocean Radar Conferences for Asia-Pacific ("ORCA"). The purpose of this web site is to provide an interim vehicle for exchanging contributions among the participants, while their final publications are being prepared. For more information, please visit the [radiowaveoceanography.org](#) and [orca2016](#) web sites.

Access is provided to the members of the ROW/ORCA community, with the understanding that no document will be redistributed or made available to third parties, without the explicit consent of their authors.

Copyright© All publications (presentations, manuscripts, texts and illustrations) found on this site are Copyright© by their respective first author. If no author is specified, the Copyright© is held by the association radiowaveoceanography.org. All rights reserved. No part of these publications may be reproduced or stored in a digital system different from the world-wide-web server www.oceanphysics.org without prior agreement with the Copyright© holder. No image embedded in these publications may be pointed to directly by other world-wide-web servers, without explicit reference to this Copyright© notice. Redistribution, whether in electronic or printed form, as well as partial use of text, figures or images in works by other authors, whether in electronic or printed form, requires written permission by the Copyright© holder. Please contact the Copyright© holders directly if you wish to use some of this material.

Cover image. The Île Vierge lighthouse, the site of the ROW-2002 field trip. Sunset picture Copyright© by [Philip Plisson](#).

row.oceanphysics.org

row2024

plymouth